4-2016

Binary metal oxides based on Fe (III) and Ti (IV) as efficient catalysts for total oxidation of volatile organic compound pollutants

Said Abdullah Sulaiman AlMamari

Follow this and additional works at: https://scholarworks.uaeu.ac.ae/all_theses

Part of the Chemistry Commons

United Arab Emirates University

College of Science

Department of Chemistry

BINARY METAL OXIDES BASED ON Fe(III) AND TI(IV) AS EFFICIENT CATALYSTS FOR TOTAL OXIDATION OF VOLATILE ORGANIC COMPOUND POLLUTANTS

Said Abdullah Sulaiman AlMamari

This thesis is submitted in partial fulfilment of the requirements for the degree of Master of Science in Chemistry

Under the Supervision of Professor Abbas Ahmed Khaleel

April 2016

Declaration of Original Work

I, Said Abdullah Sulaiman AlMamari, the undersigned, a graduate student at the United Arab Emirates University (UAEU), and the author of this thesis entitled "*Binary metal oxides as efficient catalysts for total oxidation of volatile organic compound pollutants*", hereby, solemnly declare that this thesis is my own original research work that has been done and prepared by me under the supervision of Professor Abbas Ahmed Khaleel, in the College of Science at UAEU. This work has not previously been presented or published, or formed the basis for the award of any academic degree, diploma or a similar title at this or any other university. Any materials borrowed from other sources (whether published or unpublished) and relied upon or included in my thesis have been properly cited and acknowledged in accordance with appropriate academic conventions. I further declare that there is no potential conflict of interest with respect to the research, data collection, authorship, presentation and/or publication of this thesis.

Student's Signature: _____   Date: _____

Approval of the Master Thesis

This Master Thesis is approved by the following Examining Committee Members:

1) Advisor (Committee Chair): Prof. Abbas Ahmed Khaleel

   Title: Professor of Inorganic Chemistry

   Department of Chemistry
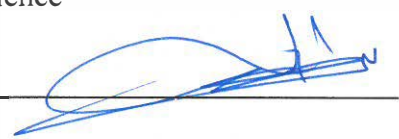
   College of Science

   Signature _____ Date 2/6/2016

2) Member: Dr. Yaser Greish

   Title: Associate Professor

   Department of Chemistry

   College of Science

   Signature _____ Date 2/6/2016

3) Member (External Examiner): Prof. Sofian M. Kanan

   Title: Professor of Chemistry

   Department of Biology, Chemistry & Environmental Sciences

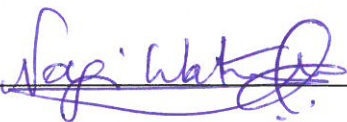   Institution: American University of Sharjah

   Signature _____ Date 1/6/2016

This Master Thesis is accepted by:

Dean of the College of Science: Dr. Ahmed Murad

Signature _____ Date 2|6| 2016

Dean of the College of the Graduate Studies: Professor Nagi T. Wakim

Signature _____ Date 2|6|2016

Copy 11 of 12

Abstract

Fe(III)-modified titania and Fe(III)-Ti(IV) binary oxides have received much less attention as possible catalysts compared to their parent single-metal oxides, Fe_2O_3 and TiO_2. This could be due to the difficulty of obtaining pure desired mono-phases. In addition, the effect of different preparative conditions on the textural properties of sol-gel-prepared Ti-Fe mixed oxides was rarely studied. Furthermore, the effect of the composition on the reducibility and the catalytic activity of these composites was never studied. In the present work, Ti-Fe mixed oxides were prepared using a modified sol-gel method and their textural properties as well as their reducibility and their catalytic activity were investigated and were compared with those of parent single-metal oxides.

The use of propylene oxides (PO) as a gelation promoter as well as the presence of hetero-ions was found to play a key role in promoting gel formation at certain concentrations. While in the presence of a single metal, colloidal solutions and very fine precipitates were obtained, gels formed readily from mixed solutions containing 5-15% Fe(III) in the presence of PO, and from solutions containing 40 and 66.7% Fe(III) even in the absence of PO.

While Fe(III) concentration as high as 10% was well dispersed in the titania lattice, which was also associated with enhanced stability of the anatase structure, higher concentrations resulted in the formation of anatase and pserudorutile (Pr) initially, which converted to rutile and pseudobrookite (Pb) upon heating at elevated temperatures. The preparation of a pure Pr phase was possible under the employed preparative conditions starting with a solution containing 40% Fe(III). However, the presence of higher concentrations resulted in the formation of some segregated α-Fe_2O_3. Xerogel and aerogel mixed oxides possessed significantly higher surface areas than their parent single metal oxides, and the surface area increased as the Fe(III) concentration increased. Furthermore, the mixed oxides showed an enhanced reducibility indicating a more labile lattice oxygen.

The mixed oxides possessed significantly improved catalytic activity compared with their single-metal oxide counterparts, especially at lower

temperatures. Using 4% air in the reaction mixture resulted in the formation small amounts of benzene besides CO_2 as the major product. However, Using 16% air in the reaction mixture, resulted in deep oxidation to CO_2 as the only product. Among the tested catalysts, TiFe67 showed the highest catalytic activity making it a promising catalyst for oxidative degradation of volatile organic compounds, VOCs.

Keywords: Sol-gel method, catalytic oxidation, iron titanates, mixed oxides, VOCs.

Title and Abstract (in Arabic)

<div dir="rtl">

أكاسيد ثنائية لمعادن انتقالية مبنية من عنصري الحديد والتيتانيوم كعوامل حفازة لأكسدة وتفكيك مركبات عضوية ملوثة للبيئة

الملخص

مركبات الحديد الثلاثي (III) Fe المضاف لأكسيد التيتانيوم، و مركبات الأكاسيد الثنائية للحديد الثلاثي (III) و التيتانيوم الرباعي(IV) تلقى اهتماما أقل بكثير كمواد حفازة مقارنة بأكاسيد المعدن الواحد، مثل أكسيد الحديد الثلاثي (α-Fe$_2$O$_3$) وأكسيد التيتانيوم (TiO$_2$). وهذا يمكن أن يكون راجعا إلى صعوبة الحصول على المركب المطلوب بنقاوة وبنية أحادية الشكل. وبالإضافة إلى ذلك، نادرا ما كان هنالك دراسة لتأثير الظروف التحضيرية المختلفة على الخصائص التكوينية للأكاسيد المختلطة للحديد و التيتانيوم بطريقة الترسيب الكيميائي المباشر سول جل (sol-gel). وعلاوة على ذلك، تم دراسة تأثير طريقة التحضير على القدرة على الاختزال والنشاط التحفيزي لهذه المركبات و التي لم تدرس من قبل. في هذا البحث، تم إعداد أكاسيد الحديد و التيتانيوم مختلطة باستخدام طريقة الترسيب الكيميائي المباشر سول جل (sol-gel) المعدلة، وجرى التحقيق من الخصائص التكوينية، وكذلك القدرة على الاختزال والنشاط الحفاز، وتم مقارنتها مع أكاسيد المعدن الواحد.

تم استخدام أكسيد البروبيلين (PO) كمحفز منظم لعملية الترسيب وكذلك وجود أيونات مغايرة تلعب دورا رئيسيا في تعزيز تشكيل الهلام (gel) بتركيزات معينة. اما عند استخدامه لتحضير معدن واحد، فقد تم الحصول على محلول رغوي به راسب ناعم جدا، في حين أعطى المواد الهلامية (gel) والتي تشكلت بسهولة من المحاليل المختلطة التي تحتوي على نسبة من 5% إلى15 % من أكسيد الحديد (III) في وجود أكاسيد البروبيلين (PO)، ومن المحاليل التي تحتوي على 40 و 66.7٪ من أكسيد الحديد (III) حتى في حالة عدم وجود أكسيد البروبيلين (PO).

عند إضافة أكسيد الحديد (III) بنسبة تركيز 10% ، نتج عنه توزع جيد في الشبكة البلورية لأكسيد التيتانيوم، و الذي ادى إلى تعزيز استقرار تركيب التيتانيوم (Anatase)، أما التراكيز الأعلى من أكسيد الحديد (III) فأسفرت في تشكيل بنيتين مختلفتين في التيتانيوم و هما (Anatase) و(Pserudorutile)، والذي تم تحويله إلى بنيتين جديدتين هما (Rutile) و

</div>

(Pseudobrookite) عند التسخين في درجات حرارة مرتفعة. و وجد أنه من الممكن تحضير بنية (Pserudorutile) نقية للأكاسيد الثنائية بنفس الظروف التحضيرية المستخدمة بدءا من محلول يحتوي على 40% من أكسيد حديد (III). ومع ذلك، فإن وجود تركيزات أعلى نتج عنه تشكيل بعض من أكسيد الحديد الثلاثي المنفصل (α-Fe$_2$O$_3$). المواد المختلطة ممكن ان تشكل نوعين من الهلام (gel) و هما الزيروجل (xerogel) و الايروجل (aerogel) و تتصف أسطح هذه الأكاسيد المختلطة بمساحة أعلى بكثير من أكاسيد المعدن الأم الواحد، بحيث تزداد كلما زادت تركيز أكسيد الحديد (III) المضاف أثناء التحضير. وعلاوة على ذلك، أظهرت هذه الأكاسيد المختلطة القدرة على الاختزال و تعزيز نفاذية الأكسجين.

تمتلك الأكاسيد المختلطة تحسن كبير في النشاط التحفيزي مقارنة مع نظرائهم لأكسيد المعادن الواحد، وخاصة في درجات الحرارة المنخفضة. فقد أدى استخدام الهواء بنسبة 4% في خليط التفاعل إلى تشكيل كميات صغيرة من البنزين إلى جانب غاز ثاني أكسيد الكربون(CO$_2$) كمنتج رئيسي. ومع ذلك، باستخدام نسبة 16% من الهواء في خليط التفاعل، أسفرت عن الأكسدة العميقة لغاز ثاني أكسيد الكربون(CO$_2$) كمنتج وحيد. كما أظهرت خليط الأكاسيد الثنائية بنسبة 67% (TiFe67) أعلى نشاط تحفيزي مما يجعله مركب حافزا واعدا لأكسدة المركبات العضوية المتطايرة.

مفاهيم البحث الرئيسية: طريقة الترسيب الكيميائي المباشر سول جل، مركبات الأكاسيد الثنائية للحديد الثلاثي (III) و التيتانيوم الرباعي(IV) ، الأكسدة بالتحفيز، الاكاسيد الثنائية، المركبات العضوية المتطايرة.

Acknowledgements

I am especially grateful to Prof Abbas Khaleel who introduced me to the exciting field of Catalysis and whose endless ideas and encouragement led to this and most other studies in which I have been involved.

I would like to thank the Graduate Program Advisory Committee for their guidance, support, and assistance throughout my preparation of this thesis. I would also like to thank the chair and all members of the Department of Chemistry at the United Arab Emirates University for assisting me all over my studies and research.

Special thanks go to my family, parents, wife, brothers, and sisters who helped me along the way. I am sure they suspected it was endless.

Dedication

To my beloved parents and family

Table of Contents

List of Tables

List of Figures

List of Abbreviations

PO	Propylene Oxide
Pb	Pseudobrookite
Pr	Pseudorutile
TB	Titanium(IV) *n*-butoxide
PrOH	2-propanol
FeNt	Iron(III) nitrate nonahydrate
XRD	X-ray diffraction
DRIFTS	Diffuse reflectance Fourier transform infrared spectroscopy
BET	Brunauer-Emmett-Teller
BJH	Barett-Joyner-Halenda
H_2-TPR	H_2-temperature programed reduction
TCD	Thermal conductivity detector
VOCs	Volatile Organic Compounds
BID	Barrier Ionization Discharge

Chapter 1: Introduction and Literature Review

1.1 Definition and Importance

Catalysts in simple term are materials that speed up reactions by lowering the activation energy without themselves being consumed in the reactions. The IUPAC definition of the word catalyst is a substance that increases the rate of the reaction without modifying the overall standard Gibbs energy change in the reaction. The cyclic process is called catalytic reaction, which due to different factors, can change the catalyst structure and may result in catalyst deactivation [1].

For many years before 1750, people used catalysts for making food and beverages. In 1746, Lead Chamber process was invented by an English man called John Roebuck to produce sulfuric acid in huge quantities by the lead chamber process. That discovery has made a significant change in the history of catalysis. Today, over 90% of the industrial chemicals and petroleum refining depend on catalysis. In addition, due to the rapidly growing industries that result in large amounts of environmental pollutants, more strict lows and controls have been in place to control polluting emissions. This is another area where catalysis started to play a key role. Therefore, various environmental catalytic systems have been investigated and many of them have shown promising performance in controlling the emission and in abatement of environmental pollutants. As a result, environmental catalysts created new business that made around one third of the revenues from catalytic materials [2,3,4].

1.2 History of Catalysts

Historically, the word catalyst came from Greek Kata, 'down' and lyein, 'loose'. Ancient Egyptians and Mesopotamians (In Iraq) made alcohol from grapes by fermentation process. In 1800, work by Joseph Priestly and Martinus van Marum lead to dehydrogenation of ethyl alcohol over metal particles. In 1813 a scientist from Paris called Claude Louis Berthollet was able to decompose ammonia by passing it over a red hot metal to give hydrogen and nitrogen gases. A year later, Pierre Dulong reported different reactions over different metals. After ten years from Louis reaction, Edmond Davy, an English scientist who worked at Cork institute, used Platinum catalyst to oxidize alcohols at room temperature. In 1918, a Nobel Prize in chemistry was granted to Haber-Bosch for his work on producing ammonia from the H_2 and N_2 using finely divided osmium. In 1835, Jacob Berzelius converted starch to sugar by acid catalysts. A year before Jacob's work, Michael Faraday worked on combustion reactions and observed that the surface of platinum metal affects the combustion process [5].

As the age of plastic emerged, many factories were working to improve such a commercial polymer. A German called Ziegler and Italian called Natta were able to develop organometallic polymerization catalysts and were awarded Nobel Prize in 1963. Other two scientists, Otto Fischer and Geoffrey, worked independently to study the organometallic sandwich compounds and their research resulted in many compounds that were have been employed as catalysts and for that, both were a worded Noble prize in 1973. After two years, the prize went to two chemists, Cornforth form England and Vladimir from Switzerland, and their

work was based on catalysis related to enzymes and stereochemistry of organic molecules.

At the beginning of 21th century, in 2001, Noble Prize was awarded to three chemists for their catalysis-related work: Knowles from USA and Noyori from Japan who explored the hydrogenation process, and the third is Sharpless who developed stereo selectivity in oxidation reactions. Two American scientists, Grubbs and Schrock, discovered transition metal catalysts for metathesis reactions, and for their interesting work they both shared Nobel Prize in 2005. Palladium-based catalysts used in organic synthesis discovered by Heck, Negishi and Suzuki lead for abundant production of complex organic molecules, and as a result they were awarded Noble Prize in 2010 [6].

1.3 Homogeneous vs. Heterogeneous

Catalytic materials can be classified as homogenous and heterogeneous catalysts. In homogeneous catalysis, the reactants and the catalyst exist in the same physical phase. In contrast, a heterogeneous catalyst exist in a physical phase different from that of the reactants, such as liquid or gas reactants and solid catalysts. Moreover, catalysts could be classified in term of the process and applications such as photo-catalysts, biocatalysts and environmental catalysts [7].

Most solid catalysts are mainly based on divided metal particles, metal oxides, metal sulfides, or transition metal complexes. Most of the catalysts employed in industry are based on metal particles and binary oxides.

The catalytic materials are very often supported on the surface of another stable, high-surface-area, and cost-effective solids such as alumina, titania, and zeolites. Many of the metal oxide catalysts are based on binary or bulk mixed

oxides as will be discussed later. Some oxides promote acid-base reactions on their surfaces while others can promote oxidation-reduction reactions. The nature of bonding in metal oxides is not fully ionic, but has ionic-covalent character that vary from one oxide to another. In addition, the surface of metal oxides very often terminate with hydroxyl groups that in many cases act as the active sites and promote different reactions. In this chapter, more consideration will be given to solid catalysts based on bulk mixed transition metal oxides.

1.4 Catalysts Based on Metal Particles

Many metals in the form of small particles, especially in the naonoscale range, have shown unique catalytic properties in various important applications. Among the important applications that depend on metal particle catalysts are hydrogenation, CO oxidation, natural gas conversions, and other energy-related applications [1-8]. The most common metal catalysts employed in these applications are Pt, Pd, Ni, Au, Ag, and Ru. Some catalysts involve two or more different metals in the form of bimetallic or poly-metallic materials. Bimetallic catalysts can be in the form of core-shell hetero-structure or alloyed structure [9]. These composite materials very often exhibit unique properties and improved performance compared with their single-metal counterparts. As an example, adding Ru or Pt metals to Ni/Al_2O_3 catalysts enhanced its performance it seam reforming reactions [10].

Similar other studies involved improvement of Ni catalysts by adding Au and Ag [11]. Other applications of metal-based catalysts include partial oxidation of methanol [12] and decomposition of organic compounds [13-14].

1.5 Transition Metal Oxide Catalysts

Transition metals have important features and properties that are, mainly, due to their *d*-orbitals electronic configuration which is associated with multi oxidation states and ability to form different metal oxides. Therefore, transition metal oxides play a significant role in various catalytic reactions, especially in oxidation processes. While in some reactions they are used in the form of single-metal oxides, in many cases, they are used as bulk mixed oxides or supported on the surface of other materials including zeolites. Bulk mixed metal oxides are widely used in different industries including petroleum industry, chemical manufacturing, and environmental applications. Because of the complexity of mixed oxide systems, their characterization and understanding of their chemistry is still a challenging task. Catalysts based on transition metal oxides include compounds and composites that involve most of the *d*-block metals as well as some metals from the *f*-block.

Transition metal oxide catalysts are generally used in oxidation processes due to their surface oxidation and reduction properties. Besides their redox properties, they may undergo acid base reactions giving importance in different types of processes. The catalytic efficiency of the metal oxides depends largely on their preparative conditions and method which, in turn, determine their textural properties and chemical behavior.

The variation in structures and surface properties of transition metal oxides allow them to be employed in a wide variety of applications. As an example, they were investigated intensively in epoxidation reactions of organic compounds and in total oxidation of volatile organic compounds (VOCs), particularly halogenated

compounds [15,16,17,18]. The metal oxides that showed promising performance in oxidation of VOCs include oxides of V(v), Fe(III), Mn(III), Cr(III), Ce(III) and Cu(II). In addition, some semiconducting transition metal oxides have been widely studied as possible photo-catalysts for oxidation and degradation of organic compounds. The most common photo-catalysts are based on ZnO and TiO_2 [19]. In the present work mixed oxide catalysts based on Ti(IV) and Fe(III) were prepared using sol-gel method and the effect of preparative conditions on the textural properties were investigated. The catalytic activity of the prepared catalysts in the oxidation of toluene was investigated.

1.6 Titanium(IV) Oxide, TiO_2

Titanium is the ninth most abundant element in the earth's crust. It was discovered in 1790, by the English man William Gregor. After 5 years, this metal was named as titanium. Titanium has low density, resistance to corrosion and has highest strength to weight ratio among all metals. Its oxide, TiO_2 (titania), has been used as a white pigment. Nowadays, titania has been widely studied in photo-catalysis, gas sensing, and in corrosion-protective coating. Moreover, it has medical uses such as in cosmetic products and bone implant.

Titanium dioxide is a white crystalline powder with 1843 ^{o}C melting point and 2972 ^{o}C boiling point, which make it thermally very stable. It is insoluble in water, but is very sensitive to moisture. Titania lattice is elementally composed of Ti cations (Ti^{4+}) surrounded by six oxygen ions (O^{2-}) in more or less distorted octahedral configuration as shown in Figure 1.1. TiO_2 crystalizes in three main phases, rutile, anatase and brookite depending on the pressure and temperature. It can also be non-crystalline in the form of amorphous powder. However,

crystalline rutile and anatase phases are more common and play significant roles in the applications of TiO_2. Anatase is less stable and convert to rutile at temperatures above 500 ^{o}C. On the other hand, rutile is more crystalline and is more thermodynamically stable. Therefore, it is the most commonly phase occurring in nature.
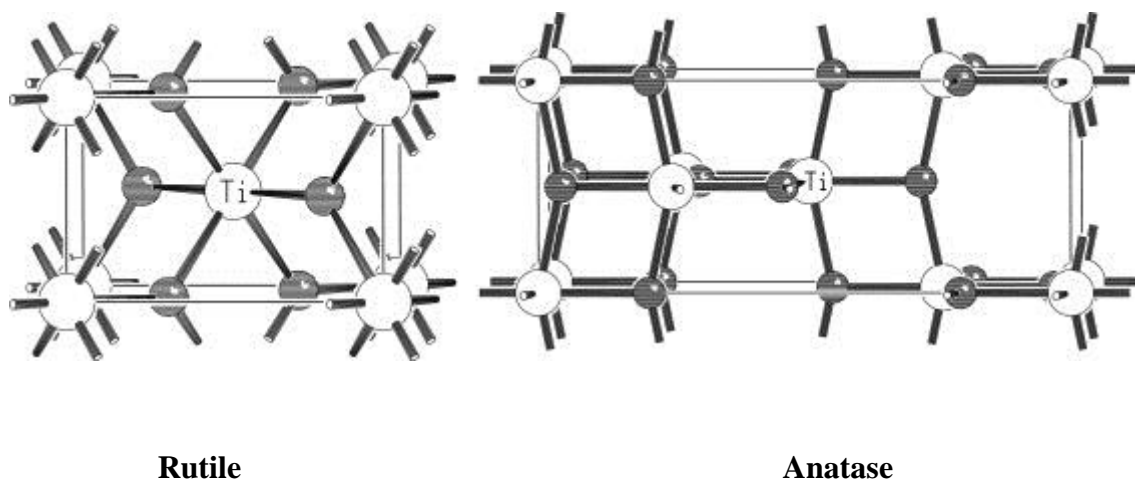
Rutile   **Anatase**

Figure 1.1 Crystalline structure of rutile and anatase [20]

The bulk of anatase TiO_2 has structure of six-fold coordination of Ti atoms that alternate with five-fold coordinated atoms. The structure has two types of oxygen, one atom with 3 coordination in the bulk and the second bridging oxygen atoms that are 2-fold coordinated. The coordinativley unsaturated sites make the anatase more active for adsorption and reactions.

Rutile has a body-centered tetragonal unit cell. It has a tetragonal system where Ti ions are octahedrally coordinated with 6 oxygen atoms. Due to that, rutile is more stable than other titania phases. Anatase can convert irreversibly to

rutile at elevated temperatures. The transition temperature of anatase to rutile depend on many factors including preparation methods, particle size and impurities. An impurity refers to the presence of other elements incorporated in the titania bulk or on the surface. The presence of such heteroatoms in titania, not only affect phase transformations, but may also affect other properties including its performance in applications [21].

1.7 Iron Oxides

Iron oxides have interesting properties and advantages including abundant availability in nature, low cost, and non-toxicity. They are widely used in industrial heterogeneous catalytic processes. They have different structures, and the most common phases include hematite (α-Fe_2O_3), maghemite (γ-Fe_2O_3) and magnetite (Fe_3O_4). Hematite is the most stable phase and is the most common phase in nature. Hematite has corundum type structure and it exhibits non-stoichiometry associated with oxygen vacancy formation. Due to acid/base properties and redox behavior, this phase of iron oxide has been used in different catalytic oxidation reactions. Furthermore, it shows semiconducting features at high temperatures.

Magnetite is the oldest type of iron oxides and is well known as lodestone. It has cubic spinel structure at room temperature. However, magnetite undergoes phase transformation above 120 °C, which is called Verwey temperature. It is used as a catalyst for industrial synthesis of ammonia.

Maghemite can be prepared by oxidation of magnetite and is known for significant redox properties due to cation vacancies in the structure. It has the

same structure of magnetite and has both octahedral and tetrahedral iron sites. Maghemite is used in sensors and magnetic applications due to magnetic and optical properties [22].

1.8 Examples of Investigated Metal Oxide Catalysts

While a metal oxide catalyst can be in the form of pure single-metal oxide, supported and mixed oxides are more common. Bulk mixed oxides are quite popular as industrial powerful catalysts since, the morphology contains different active sites, which increases their catalytic efficiency [23]. Very often, incorporating different metal ions in the same oxide matrix enhances the catalytic activity and thermal stability of the mixed oxides compared with the corresponding single-metal oxides. The chemical homogeneity depends on the composition and the chemical reactivity of the precursor of each metal ion. Catalysts based on transition metal oxides are particularly important as they exhibit different structures and magnetic properties due to the nature of d-orbital. Many of these oxides have point defects (oxygen vacancy) that are necessary for activity and selectivity in many catalytic reactions. Many metal oxides can promote oxidation catalysis by releasing lattice oxygen leaving free valences on the metal. As a result, the metal can make a second bond during chemisorption interactions. The metal oxide surface is then oxidized by molecular oxygen regenerating the surface active sites [24].

The literature is rich in examples of different bulk mixed oxides that have shown improved catalytic activity compared with single-metal oxides. The following are only selected examples. CeO_2-MnO_X and CeO_2-FeO_X exhibited

enhanced reducibility and hence improved oxidation catalytic activity [25,26]. Catalysts based on Cr(III)-Fe(III) bulk mixed oxides exhibited enhanced catalytic activity in the total oxidation of benzene [27]. ZrO_2-TiO_2 mixed oxides showed modified structural stability and enhanced reducibility [28]. Sol-gel prepared TiO_2-Al_2O_3 binary oxide showed an interesting activity in the photo-catalytic oxidation of nitrogen oxides (NO_X) which are among major environmental pollutants [29].

Catalysts based on Ti(IV) and Fe(III), which are the subject of the present work, have also received noticeable attention. As an example, sol-gel-prepared TiO_2-Fe_2O_3 binary oxides were prepared, and phase transformations were studied at various temperatures [30]. While anatase and rutile were observed at temperatures below 700 C^o, Fe_2TiO_5 phase was obtained at temperatures between 700 °C and 900 °C. The composites showed promising catalytic activity in the degradation of O-Cresol in aqueous solutions. Barojas et al [31]. Studied the photo-catalytic properties of titania, iron (III) oxide, and TiO_2-Fe_2O_3 composites in the decomposition of methylene blue under visible light illumination. It was found that the TiO_2-Fe_2O_3 mixed oxide showed higher catalytic activity than TiO_2 and Fe_2O_3 alone. M. R. Mohammadi et al. [32] studied non-crystalline TiO_2-Fe_2O_3 thin films and powders, where they prepared binary oxides for gas sensing applications since TiO_2 and Fe_2O_3 could be used as gas sensors. This property is due to their electrical conductivity change upon reaction with exposed gases such as CO, O_2 and H_2.

The surface nature of the bulk mixed oxides is complicated due to possible different oxidation states and variable coordination. Also, the presence of oxygen

atom vacancies in the bulk complicates the surface morphology [22]. The surface nature of the outermost layer of bulk mixed metal oxide was difficult to be understand until recent development of several advanced techniques and instruments for surface characterization.

1.9 Environmental Applications of Heterogeneous Catalysts

The fast developments and the trends in modern life are associated with considerable negative impact on the environment putting the quality of life in a serious risk. Industrial activities and transportation are major sources of environmental pollution. Increasing the public awareness and taking all measures possible to reduce pollution are becoming two major global concerns to ensure sustainable environment. Therefore, developing efficient catalysts for emissions' control and pollutants abatement is becoming a real challenge for researchers and scientists working in the field of environmental catalysis. It has been found that heterogeneous catalysts can offer solutions to many environmental problems, especially in relation to emission control and degradation of pollutants. This includes control of air, as well as water, pollutants such as carbon monoxide, nitrogen oxides, sulfur oxides, and VOCs.

VOCs are organic materials that have high vapor pressure at ordinary room temperature conditions. According to World Health Organization, VOCs are organic compounds with boiling points in the range of 50-260 °C, including indoor and outdoor compounds. The indoor VOCs emission can originate from cooking, furniture, cleaning supplies, paints and office equipment. Nowadays, people spend more than 80 % of their time close to these sources either at home or at work. Outdoor sources include transportation, oil and almost all industries [33].

VOCs have various serious effects on the environment in general and on human health in particular. VOCs have been found to be responsible for health problems such as respiratory distress, eye problems, throat irritation and cancers. Some VOCs also cause ozone depletion, and contribute to the problem of global warming.

1.10 VOCs Catalytic Degradation

Catalytic combustion of VOCs has been found to be a promising technique to reduce the emission of these compounds. There has been a significant amount of research on developing catalysts for environmental applications, especially VOCs oxidative degradation. Two type of catalysts have been widely investigated and employed for this purpose: (1) Catalysts based on noble metals such as Pt and Pd, and (2) catalysts based on transition metal oxides. The catalytic activity of transition metal oxides can be as good as that of noble metal catalysts [34]. Moreover, transition metal oxide catalysts offer significant advantages over metal catalysts which are usually associated with high cost, severe sintering, and rapid deactivation at high temperatures. On the other hand, metal oxide catalysts are more cost-effective, more thermally stable against sintering, and can be easily prepared in high surface areas.

The examples described below are selected examples from the literature on catalysts based on transition metal oxides and their activity in VOCs abatement. Mutin et al.[34] reported an interesting catalytic activity for Vanadia-Titania catalysts in the total oxidation of benzene as an example of aromatic pollutants. They found that the performance of the catalysts was largely dependent on the catalyst composition and the nature of vanadium surface species. Zou et al. [35]

investigated the effect of silica in nanostructured TiO_2-SiO_2 pellets on the ability of removing toluene by photo-catalysis. A mesoporous powder of CuO-CeO_2 showed interesting catalytic activity for total oxidation of benzene as reported by Zhu et al.[36]. It was found that the nature of the active sites on the surface was dependent on the calcination temperature and the activity was enhanced due to high surface area and porosity of the catalysts. In a recent study, several catalysts based on different transition metal oxides supported on titania (MO_x/TiO_2 where M= Mn, Ce, Co,Fe) were investigated in the oxidation of benzene at temperatures between 100 °C and 450 °C. The study found that MnO_x/TiO_2 catalysts showed the highest activity and its performance was dependent on the manganese loading where the optimum loading was 5% [37].

1.11 Preparation Methods of Metal Oxide Catalysts

There are several well-established preparative methods for metal oxides. These methods include hydrothermal, co-precipitation, and sol-gel methods. These methods can be used to prepare single-metal or mixed metal oxides. For supporting a metal oxide on another material, wetness impregnation has been the most widely used method. Hydrothermal synthesis is used for the synthesis of crystalline metal oxides using metal precursors dissolved in water and the reaction mixture is pressurized in a high-temperature high-pressure reactor [38]. The co-precipitation method is usually used to prepare mixed oxides. In this method, appropriate amounts of solutions of different metal precursors are mixed and the pH of the mixture is adjusted to allow precipitation of mixed metal hydroxide or oxide composite. The separated solid is then claimed at appropriate temperatures to obtain the final desired product [39].

Sol-gel method is another widely used method for preparation of metal oxides. It offers several advantages over the other methods including the possibility of producing powders with high surface areas and high porosity. In addition, it can lead to mixed oxides with good homogeneous mixing and well dispersion of dopant ions. The starting material of the precursor is usually a colloidal solution (sol) of an alkoxide or an inorganic salt precursor of the studied metals. The precursor undergoes condensation reactions resulting in a polymeric network that contains the solvent in the form of a gel. This method was selected for the preparation of the catalysts in the present work and more description will be given in chapter 2.

In wetness impregnation method, which is the most widely used method for preparing supported oxide catalyst, the active phase precursor is dissolved in an appropriate solvent and the solution is added to a pre-prepared powder of the support. The amount of the active phase solution is determined carefully to obtain the desired loading and so that the solution is just enough to fill the pores of the support material. After well mixing, the paste-like mixture is dried and then the solid is calcined at an appropriate temperature [40].

1.12 Catalyst Deactivation

Catalytic activity and selectivity are two important criteria that determine the efficiency and suitability of a catalyst. During the catalytic reaction, different factors can affect these properties and may change the structure and the efficiency of the catalyst. The first common factor is poisoning which results from strong chemisorption of contaminate species. The adsorbed species can block the surface active sites on the catalyst. The second factor is thermal deactivation or sintering

which is usually a consequence of employing elevated temperatures. Sintering results in a considerable decrease in the surface area and porosity which eventually decrease the number of surface active sites [7].

1.13 Research Problem and Objectives

The preparation of nanostructured porous Fe(III)-modified titania and Fe(III)-Ti(IV) binary oxides has not received enough attention from researchers. Monophasic Fe(III)-Ti(IV) oxides, in particular have not been studied enough, which can be referred to the difficulty in obtaining pure phases. Furthermore, no studies are reported on the possibility of employing these binary oxides in oxidation catalysis. Therefore, the main objective of the present work is to study the preparation of such materials using modified sol-gel method in order to prepare porous nanostructured powders of these solids. The second main objective is to study the performance of these materials as catalysts in the oxidation of volatile organic compounds which are considered among main sources of environmental pollution.

Chapter 2: Preparation and Characterization of Fe(III)-Modified Titania and Fe(III)-Titanates

2.1 Introduction

Metal oxide composites exhibit interesting properties and promising performance in a wide range of applications including catalysis, ceramics, and magnetic materials. Therefore, they have attracted significant attention as promising materials in different advanced applications. The presence of a foreign element in the matrix of a metal oxide can greatly modify its structure and properties including mechanical, chemical, and textural properties. Catalysis is one of the applications where mixed metal oxides have shown very interesting behavior and modified performance as compared to single-metal oxides.

Titanium-iron oxides, in particular, have attracted significant attention due to their possible enhanced performance in various applications including semiconductors, ferromagnetic materials, ceramics, and catalysis. They naturally occur in different structures and represent an important source of iron and titanium elements. They include a variety of binary oxides with different compositions including ilmenite ($FeTiO_3$), pseudobrookite (Fe_2TiO_5), pseudorutile ($Fe_2Ti_3O_9$) ulvöspinel-magnetite ($Fe_{3-x}Ti_xO_4$), and ilmenite-hematite ($Fe_{2-x}Ti_xO_3$) [52]. Due to their importance in various applications and the different behavior of different phases, preparation of these materials with modified textural and chemical properties, especially pure single phases, would be of great interest. Based on the different literature reports, it seems that getting a pure single phase of Fe(III)-Ti(IV) based compounds is challenging due to easy thermal transformations between these compounds and their corresponding single-metal oxides. It has

been noticed that, regardless of the method of preparation, Ti(IV)-Fe(III) mixed oxides decompose into rutile and pseudobrookite phases as final stable compounds at elevated temperatures [46,52]. As an example, when nanostructured 1-D titania was doped with Fe(III) substituting octahedral Ti(IV) ions, the structure was stable at temperatures as high as 400 ^{0}C and decomposed to pseudobrookite and rutile at higher temperatures. Similarly, the oxidation of ilmenite was found to result in rutile and pserudobrookite upon heating at temperatures above 700 °C [53,54].

Compared to their parent single metal oxides, which were investigated widely as catalysts in different types of reactions, Fe(III)-modified titania and Fe(III)-Ti(IV) binary oxides have received much less attention as possible catalysts. This could be due to the difficulty of obtaining pure desired phases. Their possible potential as catalysts could stem from the presence of metal ions of different oxidation states which may enhance the presence of defect sites or structural hydroxyl groups leading to new surface active sites and different acid-base as well as redox behavior. In addition, the effect of different preparative conditions on the textural properties of sol-gel prepared Ti-Fe mixed oxides was rarely studied. Furthermore, the effect of the composition on the reducibility of these materials, which is an important measure to evaluate their potential in oxidation catalysis, was never studied. These expected properties were the driving force behind this present work where Ti-Fe mixed oxides were prepared using a modified sol-gel method and their textural properties as well as their reducibility were investigated and were compared with those of parent single metal oxides.

2.2 Experimental

2.2.1 Materials and Preparation

Iron(III) nitrate nonahydrate (Fe(NO$_3$)$_3$.9H$_2$O, 98%), titanium(IV) *n*-butoxide (Ti(OBu)$_4$, 97%), 2-porpanol (99.7%), and propylene oxide (99%) were purchased from Aldrich and were used as received. Ti(IV)-Fe(III) mixed oxides, referred to as TiFeX where "x" represents the molar %Fe(III), were prepared by sol-gel method using Ti(OBu)$_4$ (TB) and Fe(NO$_3$)$_3$.9H$_2$O (FeNt) in 2-propanol (PrOH) as the solvent. Figure 2.1 presents a scheme of the general steps involved in the preparation. Composites with different iron concentrations were prepared by starting with appropriate amounts of both precursors in the starting solutions. The precursors of both metal ions were dissolved separately in PrOH. TB was dissolved in PrOH in a PrOH:TB v/v ratio of 5:1 and FeNt was dissolved separately in the same solvent (around 20 mL PrOH/g FeN). The FeNt solution was added to the TB solution and propylene oxide (PO) was immediately added to the mixture. PO/FeN+TB molar ratio was 10:1. As an example, in the preparation of TiFe10, 6.0 mL (0.0176 mol) of TB was dissolved in 40 mL PrOH and 0.792 g (1.96 x 10^{-3} mol) FeNt was dissolved separately in 60 mL PrOH. After mixing both solutions, 15 mL PO was added and the mixture was stirred for 3 hours. The reaction mixture was aged for 24 hours where gel or a colloid/precipitate mixture was obtained depending on the composition as discussed below. The solvent was removed by evaporation in a water bath at 80 °C and the obtained products were further dried in an oven at 120 °C for 1 h before calcination at 350 ºC for 1 hour and at 500 °C for 4 hours giving light-dark brown powders. Single metal oxides, titania and iron oxide, were prepared by the same method.
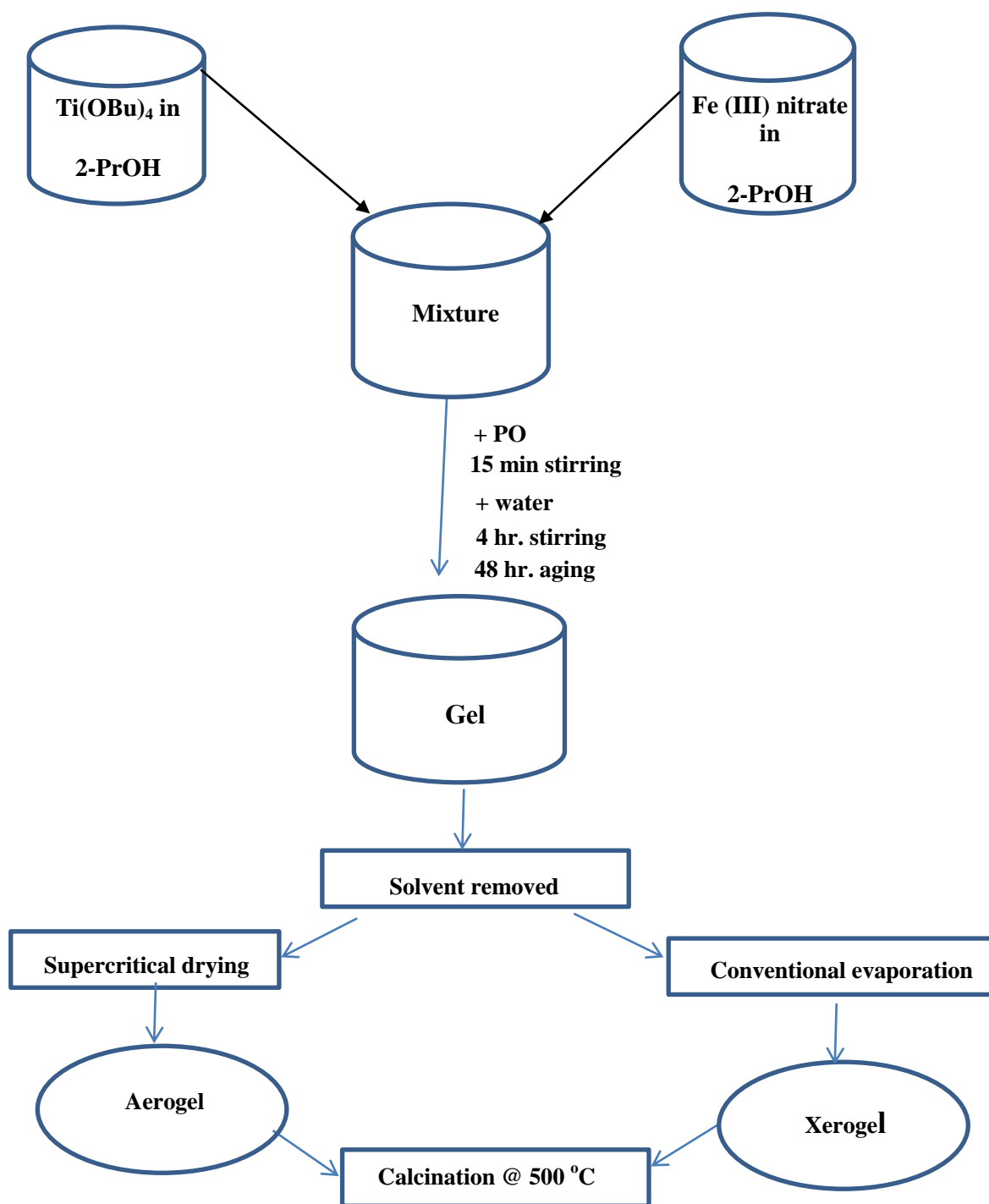
Figure 2.1: A scheme of the main steps of the preparation of Fe-Ti oxide composites

2.2.2 Characterization

The products were characterized by powder X-ray diffraction (XRD), diffuse reflectance Fourier transform infrared spectroscopy (DRIFT), N_2 adsorption, and H_2-temperature programed reduction (H_2-TPR). XRD analysis was performed on a Shimadzu-6100 powder XRD diffractometer with Cu-K_α radiation, $\lambda = 1.542$ Å. Diffraction data were collected in the 2θ angle range of 20-85 degrees at a rate of 2 degrees/min. DRIFT spectra were recorded on a Shimadzu IR-Affinity-1 spectrometer in the wavenumber range of 400-4000 cm^{-1} at a resolution of 4 cm^{-1}. The spectrometer was equipped with DRIFT accessory, from Pikes Technologies, with a heated cell that could be heated in-situ at temperatures as high as 900 ºC. KBr powder mixtures (10% by mass) were used and a background spectrum was recorded for KBr at 25 ºC after pretreatment at 150 ºC under nitrogen flow, 10 mL/min, for 30 min. The samples were then heated under the same N_2 flow to 500 °C and spectra were collected at different temperatures where the sample was soaked for 20 minutes at each temperature before recording the spectrum.

N_2 adsorption studies at 77 K for surface area and porosity measurements were conducted on a Quantachrome Autosorb-1 volumetric gas sorption instrument. Samples were degassed at 150 °C for one hour before measurements. The surface area was obtained by the Brunauer-Emmett-Teller (BET) method and the pore size distributions were determined by Barett-Joyner-Halenda (BJH) model from the desorption branch of the N_2 isotherms.

H_2-TPR experiments were carried out on a Quantachrome ChemBET TPR/TPD instrument. In each experiment, 70 mg sample was placed in a U-shaped Pyrex tube and was degassed at 300 °C for 30 minutes in N_2 at a flow rate of 30 mL/min. After cooling to 100 °C, the sample was heated to 900 °C at a rate

of 30 °C/min under the flow of the reducing gas mixture, 5% H_2 diluted in N_2, at a flow rate of 50 mL/min. The H_2 uptake during the reduction was measured by a thermal conductivity detector, TCD.

2.3 Results and Discussion.

2.3.1 Gel Formation

The sol–gel process is a widely used wet-chemical technique for the preparation of metal oxide materials especially when nanostructured porous materials are desired. Therefore, it is very often employed to prepare metal oxide-based catalytic materials for various applications. In sol-gel preparation, the starting precursor is, generally, a colloidal solution, sol, which is basically a stable dispersion of colloidal particles in a solvent. The colloidal solution then undergoes condensation reactions resulting in the formation of a gel which is basically a three dimensional continuous network of either discrete particles or network polymers that encloses a liquid phase. If the network is built from the agglomeration of colloidal particles, it is referred to as a colloidal gel. On the other hand, if the gel is based on a polymeric network of connected sub-colloidal particles, it is referred to as polymeric gel. The interactions between the components of the gel network are very often covalent in nature and therefore the gel formation is an irreversible process in this case.

For most of the sol-gel prepared materials, metal alkoxides are used as typical precursors. However, iron alkoxides are very unstable and therefore are not readily available. Therefore, we used hydrated Fe(III) nitrate as iron precursor and Ti(IV) *n*-butoxide as the titanium precursor. Starting with a metal inorganic

salt does not give a gel readily and therefore, PO was used in the current study as a gelation promoter and its role is discussed below.

The presence of PO as well as the presence of hetero-ions were found to play a key role in promoting gel formation at certain concentrations as shown in Table 2.1. However, the role of PO was also affected by the presence of excess water in the solution. It was noticed that when excess water is present, the PO does not work effectively as a gelation promoter. This can be referred to the reaction of PO with water resulting in ring opening forming propyl alcohol. This effect was confirmed by testing solutions containing single metal ions where water was added to the solutions in a water/metal molar ratio of 5.

In the absence of water, hydrolysis reactions would proceed utilizing the water in the hydrated iron precursor. However, in the case, of Ti(IV)-only, water was added since no water is available in its precursor and no reaction was observed in the absence of water. Therefore, in all preparations, other than pure titania, no additional water was used.

While in the presence of single metal colloidal solutions and very fine precipitate were obtained, interestingly, gels were readily obtained from mixed solutions containing 5-15% Fe(III) in the presence of PO. On the other hand, concentrations of 20% Fe(III), under the same conditions, resulted in some precipitation. However, when iron concentration was increased to concentrations between 40 and 66.7%, (which is referred to as TiFe67), gels formed readily.

On the other hand, no homogeneous gels formed from mixed metal solutions containing 5-20% Fe(III) ions in the absence of PO. Instead, colloid-precipitate mixtures were obtained and the amount of precipitate increased as the iron concentration increased. However, concentrations of 40-67% in the absence

of PO resulted in gel formation upon aging for around 3 days. Table 2.1 summarizes the observations in terms of gel formation from the different compositions in the presence as well as in the absence of PO. These results indicate that the gel formation depends on both, the presence of PO as well as on the concentration of Fe(III) ions in the solution. Unless otherwise mentioned, the products discussed throughout this chapter are prepared in the presence of PO.

Table 2.1: Summary of gel formation in the presence vs. the absence of propylene oxide

Composition	Gel formation or precipitation	
	Presence of PO	Absence of PO
TiO_2	Colloid-Precipitate	Precipitate
α-Fe_2O_3	Colloid/ very fine precipitate	Precipitate
TiFe5	Gel	Colloid-gel
TiFe10	Gel	Colloid-precipitate
TiFe15	Gel	Colloid-precipitate
TiFe20	Colloid-precipitate	Colloid-precipitate
TiFe40	Gel	Gel
TiFe50	Gel	Gel
TiFe67	Gel	Gel

PO oxide is known to act as a proton scavenger where its molecules abstract protons from the dissolved meal aqua-complex ion intermediates ($[M(H_2O)_x)]^{n+}$, (M = Ti and/or Fe). The deprotonation results in hydroxo/aqua complex ions ($[M(OH)_x(H_2O)_{6-x}]^{+n-x}$) which condense to form oxide/hydroxide sol particles. The sol particles condense further to form the gel. This process is known to be promoted as the pH of the solution increases due to the abstraction of protons by PO. The protonated PO undergoes an irreversible ring-opening reaction with the nucleophilic ions in the solution. However, the nucleophilic nature of nitrate ions may not be enough for the epoxide ring opening and therefore reaction with water, a stronger nucleophile than nitrate ions, may compete leading to 1,2-propanediol as a result of interaction with ring carbons. This process regenerates a proton in the solution and therefore the pH does not change significantly. However, the nucleophilic nature of the nitrate ion is enhanced in non-aqueous media and may promote ring-opening reaction of the PO. This reaction would lead to 1- and 2-nitrooxy-2-propanol ($CH_3CH_2(ONO_2)CH_2OH$) as shown in Figure 2.2. In addition, we believe that the absence of excess water, by avoiding additional water to the reaction mixture, relying only on water molecules in the hydrated precursor as a source of water for hydrolysis, enhanced the interaction of PO with the metal ion intermediates and the nitrate ion in the ring opening reaction. This may explain the fact that no gel formed from the solution of titanium precursor alone in the presence of PO where water had to be added for hydrolysis. Although no additional water was added to the solution of Fe (III) nitrate alone, it did not form a real gel but instead it gave a colloid and very fine precipitate. However, it did form a gel in ethanol as tested in

a separate study, and is not discussed further in the present work, which indicates an effect from the solvent that needs further investigation.

$$M^{n+} + H_2O \longrightarrow [M(H_2O)_6]^{n+}$$

$$[M(H_2O)_6]^{n+} \downarrow$$

$$H_3C-\overset{\displaystyle OH}{\underset{\displaystyle CH_2ONO_2}{|}} + [M(OH)_x(H_2O)_{6-x}]^{(n-x)+}$$

$$\downarrow$$

$$Gel$$
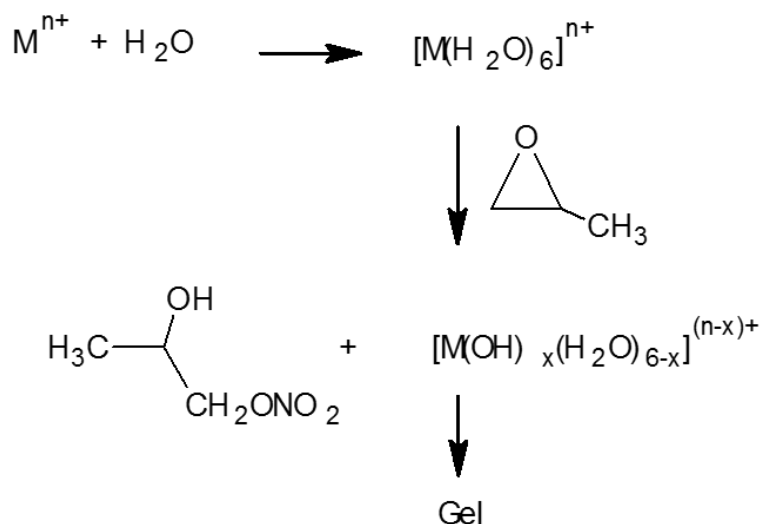
Figure 2.2: A schematic representation of the gel formation process

Interestingly, the presence of 5-15% Fe^{3+} in the titanium precursor solution resulted in the formation of gel readily indicating a key role of the iron ions in the gel formation process. The role of the iron ions could be referred to their ability to coordinate to the surface of the sol particles of titania intermediates acting as linkers to form a network and hence preventing particle growth and precipitation. However, at Fe^{3+} concentration of 20%, less homogeneous mixture was obtained and some precipitation was observed. This could be referred to the presence of excess iron ions allowing the segregation of iron species. On the other hand, in the cases of Fe concentration of 40-67%, almost no precipitation was observed and instead, gels formed. This could be referred to the high concentration of both metal ions which, due to well mixing in solution, prevented segregation and precipitation of single-metal species. Instead, these conditions provided the

chance for the development of binary oxide phases which was evident from the XRD results as discussed below.

2.3.2   Structural Characterization

Figure 2.3 displays the powder XRD patterns of the single- and mixed-metal oxide products with Fe(III) concentrations of 5-20% after calcination at 500 °C. The pattern of Ti(IV)-only product indicated the formation of anatase TiO_2, with a trace of rutile phase, and that of Fe(III)-only product indicates the formation of α-Fe_2O_3. The structure and the crystallinity of the composite products were dependent on the concentrations of both metal ions. It is evident that the presence of iron ions, generally, hindered the formation of rutile phase and almost only crystalline anatase TiO_2 structure was observed. As the concentration of Fe(III) increased, the anatase peaks became broader and weaker confirming the dispersion of the iron ions in the titania structure.
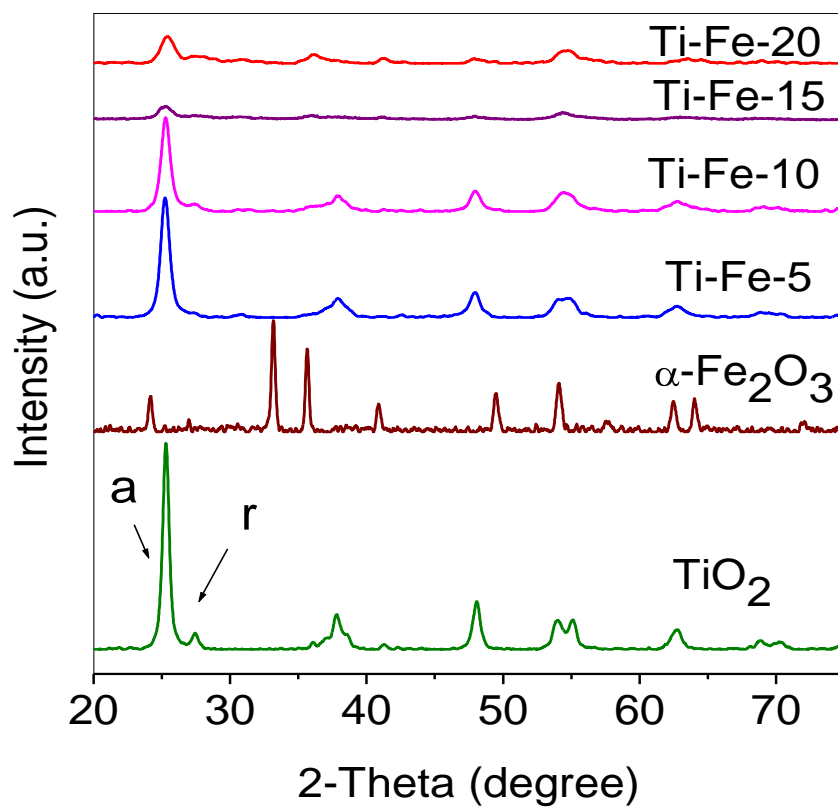
Figure 2.3: XRD pattern of TiFe5-20 calcined at 500 °C compared with single metal oxides. a and r refer to anatase and rutile, respectively

Besides the dominant anatase phase in TiFe15 and TiFe20, the formation of other phases is evident as indicated by the weak diffractions at 2θ of 30° and 36° in addition to relatively stronger diffraction at 2θ of 54°. These features, more likely, indicate the formation of pseudorutile (Pr), $Fe_2Ti_3O_9$, (JPCDS 19-0635) which is usually very poorly crystalline and difficult to characterize [54]. However, its formation becomes more evident as the samples were heated at elevated temperatures as discussed below. These results indicate that Fe(III) in a concentration as high as 10% can be well dispersed in the TiO_2 lattice, and new Fe-containing phases start to form at higher Fe(III) concentrations.

To better characterize the products, the solids were calcined at elevated temperatures, 600 and 700 °C, where the crystallinity of all phases present in the products is significantly enhanced as shown in Figure 2.4. While TiFe5 and TiFe10 contained only TiO_2 phases at 700 °C, TiFe15 and TiFe20 showed diffraction peaks that clearly represent pseudobrookite (Pb), Fe_2TiO_5, (JPCDS 41-1432) which is usually highly crystalline and easy to characterize. The formation of Pb and the absence of α-Fe_2O_3 at elevated temperatures further confirms that the Fe-containing phase at 500 °C was Pr as suggested above, where Pb resulted from the decomposition of Pr to Pb and rutile upon heating at elevated temperatures. This transformation is also supported by similar observations in composites with higher iron concentrations as discussed below. In addition, the diffraction patterns of TiFe5 and TiFe10 showed a shift in the anatase 101 and rutile 110 peaks to lower angles after they were heated at 700 °C, as shown in Table 2.2 and Figures 2.5. These observations indicate a noticeable lattice distortion confirming the incorporation of the iron ions in the titania lattice upon

Table 2.2: Shift in rutile diffraction peak positions and lattice d-spacing at 700 °C

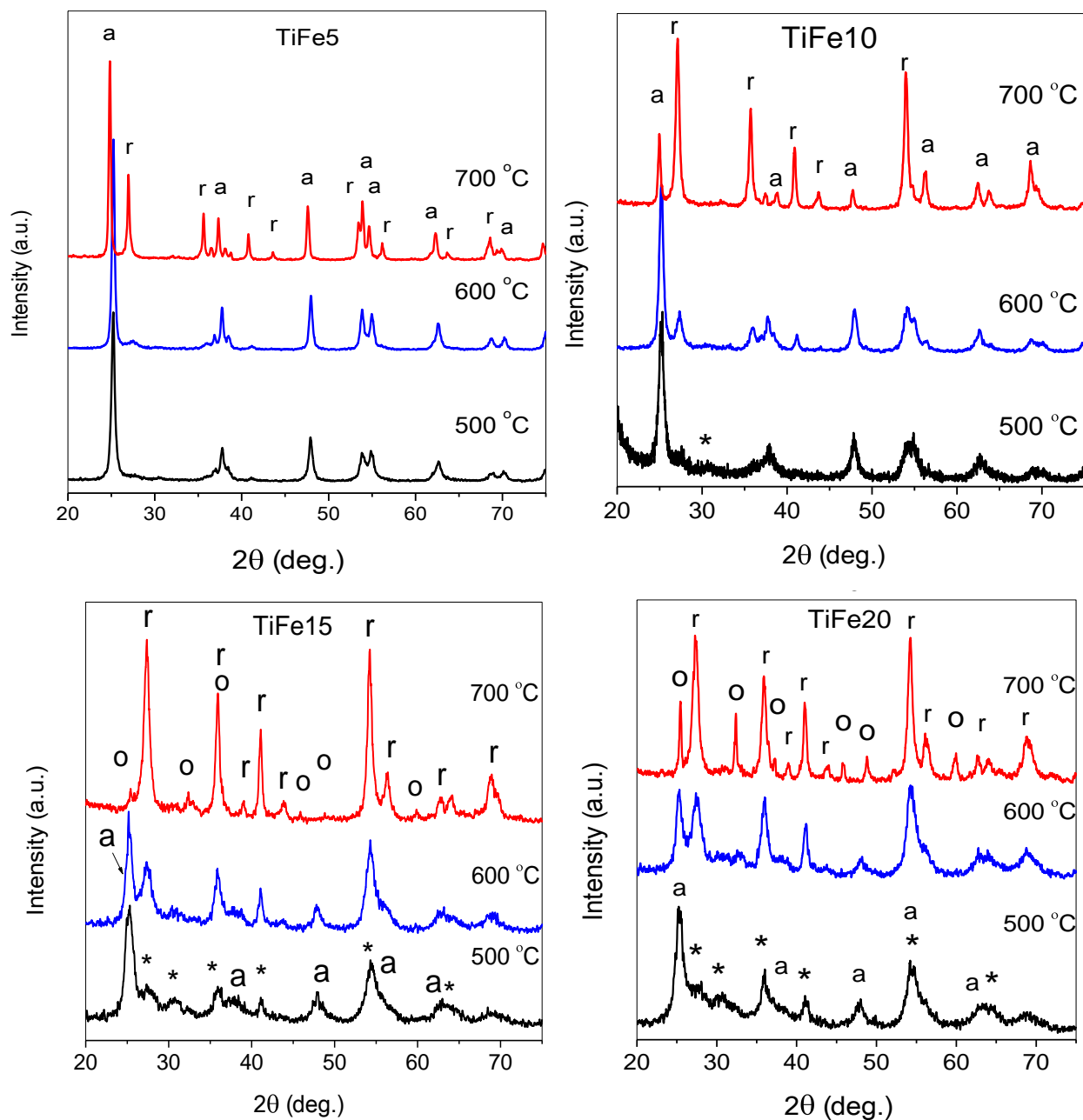| Composite	$\Delta\ 2\theta$	$\Delta\ d$-spacing
TiFe5	0.413	0.049
TiFe10	0.270	0.032
TiFe15	0.083	0.010
TiFe20	0.050	0.006
TiFe40	0.005	0.001
TiFe67	0.08	0.01

Figure 2.4: XRD patterns of TiFe5-20 after calcination at different temperatures

a: anatase, r: rutile,*: pseudorutile, o: pseudobrookite

heating at elevated temperatures. Since the peak shift was observed only at 700 °C may indicate that at lower temperatures, 500 and 600 °C, some amorphous Fe(III) species formed initially, probably on the surface of the titania particles, and further heating to 700 °C lead to incorporation of the Fe ions in the titania lattice as shown in the scheme presented in Figure 2.6.

The presence of very week diffraction features in the XRD pattern of TiFe10 that represent Pr which disappeared at 700 °C may confirm this suggestion. Surprisingly, TiFe5 showed a noticeably larger peak shift than TiFe10 indicating enhanced lattice distortion. This behavior is still not well understood, especially that more iron is incorporated in the titania matrix of TiFe10 as indicated by its broader diffraction peaks and smaller crystallite size as will be discussed below.

On the other hand, no significant peak shifting was observed in the cases of TiFe15 and TiFe20 as shown in Table 2.2 and Figure 2.6. These observations indicate that as the iron ions concentration increases a binary oxide formation becomes favored over incorporation of iron ions in the titania lattice. This suggestion is further confirmed by observing the same behavior, where no significant shift was observed, in cases of higher iron concentrations, TiFe40 and TiFe67 which will be discussed below.
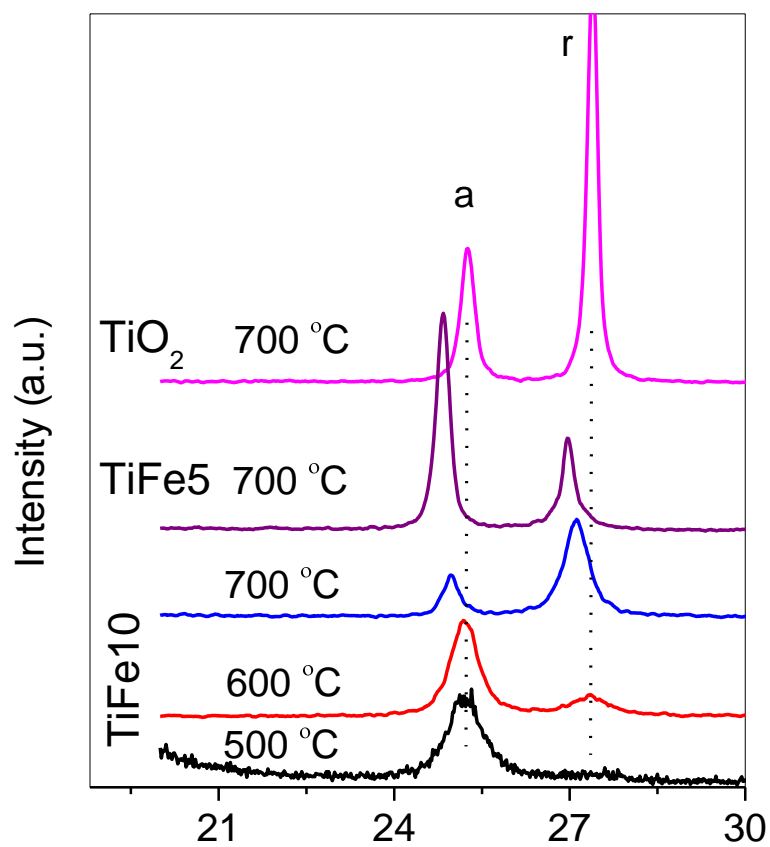
Figure 2.5: Peak shift in the anatase and rutile main peaks of TiFe10 compared with pure TiO_2. a: anatase, r: rutile
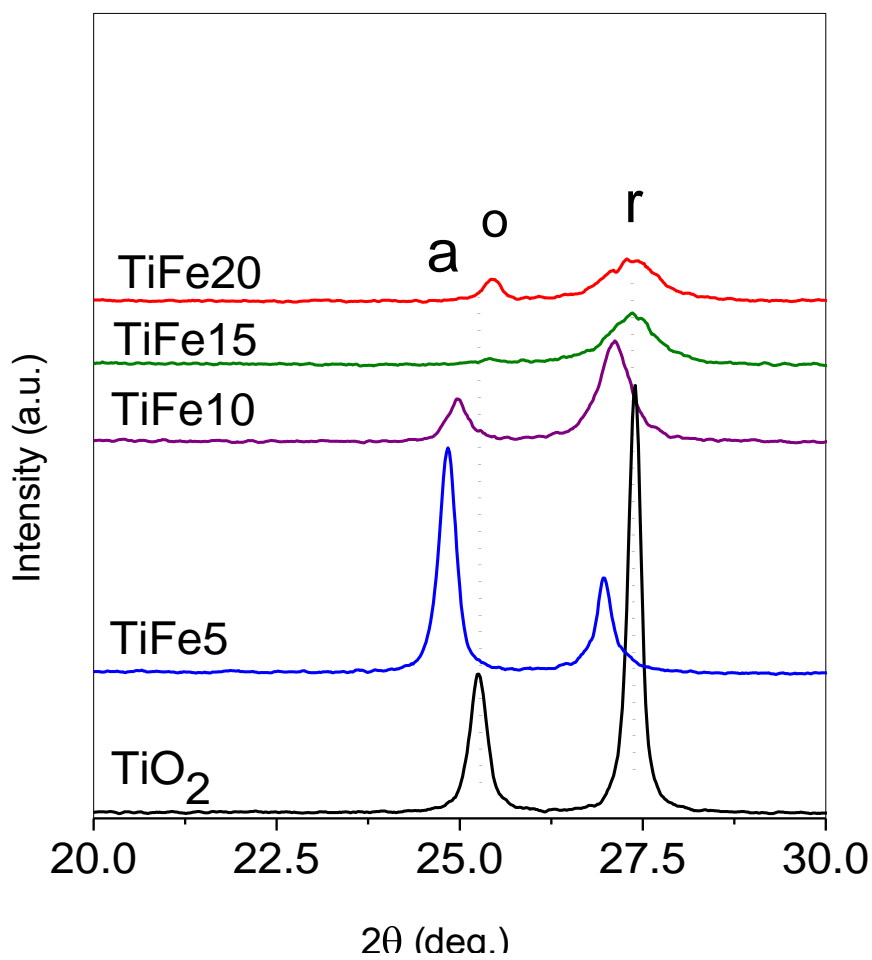
Figure 2.6: Peak shift in the anatase and rutile main peaks of TiFe5-20 compared with pure TiO_2. a: anatase, r: rutile, o: pseudobrookite

The iron ions incorporated in the titania lattice as well as the presence of binary oxide phases generally hindered the crystallization and the crystal growth as inferred from the peak broadening in the XRD patterns. The crystallite sizes calculated using Scherer equation based on broadening of the anatase or rutile peaks are shown in Table 2.3. In addition, the Fe concentration had a significant effect on the TiO_2 anatase conversion to rutile upon heating as shown in Figures 2.4-2.7. It is evident that the iron concentration of 5% stabilized the anatase structure against transformation to rutile at elevated temperatures. Based on the observations discussed above it can be concluded that (1) Fe(III) concentration below 10% can be well dispersed in the titania lattice before binary oxide phases can form. (2) Iron concentration lower than 10% can be used to enhance the stability of the anatase phase. (3) Upon calcination at temperatures up to 600 °C, Fe(III) higher than 10% result in the formation of anatase and Pr which convert to Pb and rutile at higher temperatures.
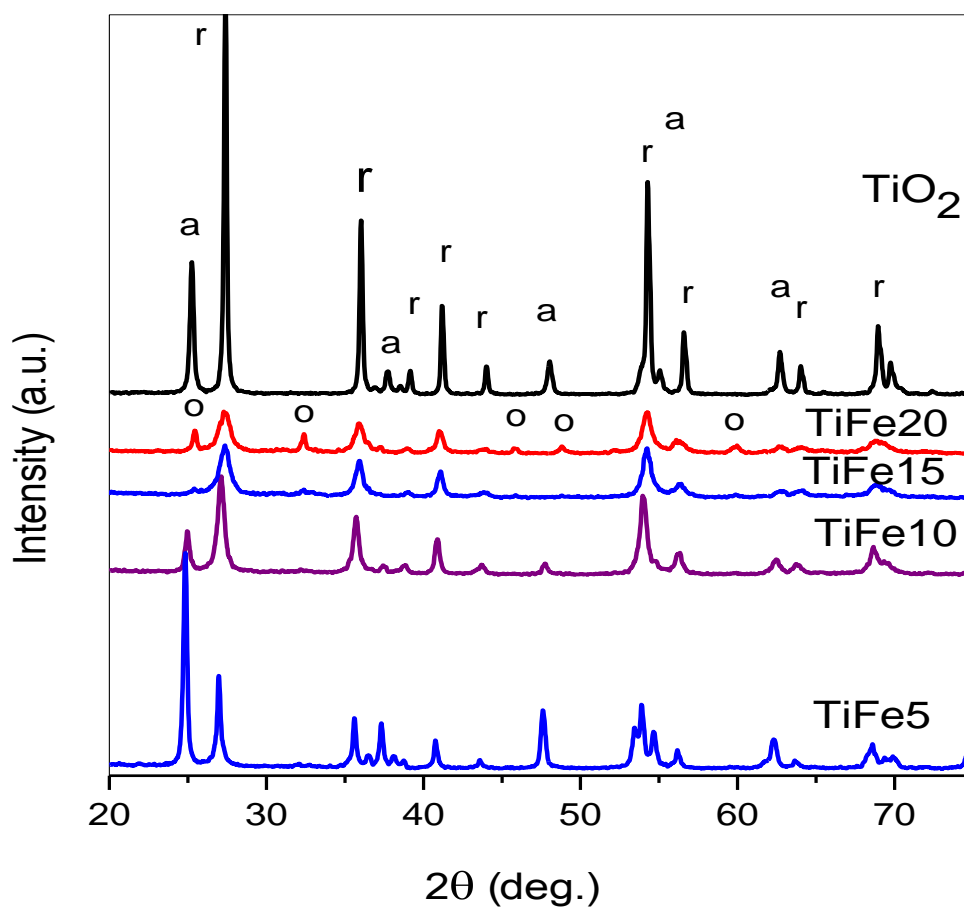
Figure 2.7: XRD patterns of TiFe5-20 and TiO_2 after calcination at 700 °C. a: anatase, r: rutile, o: pseudobrookite

Table 2.3: Crystal sizes of TiFe oxide composites and single metal oxides after calcination at 500 and 700 °C

Composition	Crystal size (nm)	
	500 °C	700 °C
TiO_2	18	45
TiFe5	22	34
TiFe10	12	19
TiFe15	7	13
TiFe20	11	17

The preparation of monophasic Ti-Fe binary oxides of Pr and Pb from solution mixtures containing the appropriate stoichiometric concentrations of Fe(III) and Ti(IV) was also investigated. The molar concentrations of Fe(III) in the starting solutions were 40% and 66.7%, representing the concentrations in Pr and Pb, respectively, and will be referred to as TiFe40 and TiFe67. The XRD patterns of the products after calcination at different temperatures are shown in Figures 2.8 and 2.9. After calcination at 500 °C, Figure 2.8, no significant diffraction was observed indicating amorphous powders, especially in the case of TiFe67. Further calcination at 600 and 700 °C resulted in noticeable crystallization. Although TiFe40 has the exact Fe/Ti ratio in Pr, it showed patterns for a mixture of Pb, and Pr after calcination at 600 °C. However, the product of TiFe67, which contains the iron concentration in Pb, was mainly Pr and only a trace of Pb was observed. On the other hand, calcination at 700 °C resulted in

rutile and Pb as the main phases in both products. In addition, however, TiFe67 contained some α-Fe_2O_3. .

These observations encouraged us to investigate the product of a composite containing equal molar concentrations of both metal ions, TiFe50, to see if free iron oxide would form. Its XRD patterns at different calcination temperatures are shown in Figure 2.10, where only features that represent Pr were observed at 500 °C and a mixture of Pb and Pr were present at 600 °C. Since the iron concentration in the starting solution was more than that in Pr, the product at 500 °C must contain, in addition to the observed Pr, iron-containing amorphous phases such as Fe-doped anatase and Pb. This may explain the noticeably higher concentration of Pb at 600 °C compared to the other composites discussed above, which resulted in higher concentration of Pb at 700 °C on the account of rutile. Interestingly, no segregated α-Fe_2O_3 was observed at any temperature indicating that a concentration of 50% Fe(III) can be used without the formation of segregated single metal oxides, and a mixture of Pr and Pb can be obtained after calcination at temperatures as high as 600 °C, beyond which the Pr decomposes to Pb and rutile. Based on the observations discussed above, the main phases detected in the different composites are summarized in Table 2.4.
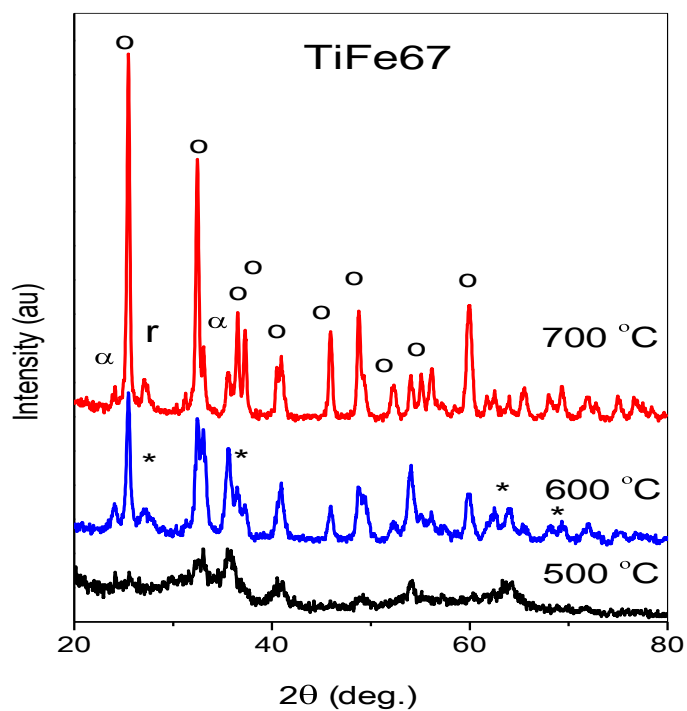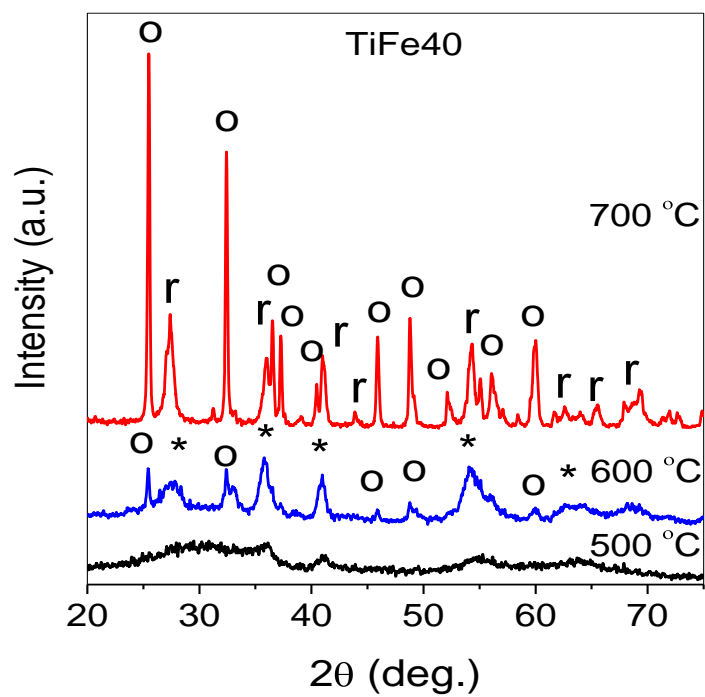
Figure 2.8: XRD patterns of TiFe40 and TiFe67 at different temperatures. *: pseudorutile, o: pseudobrookite, r: rutile, α: α-Fe$_2$O$_3$
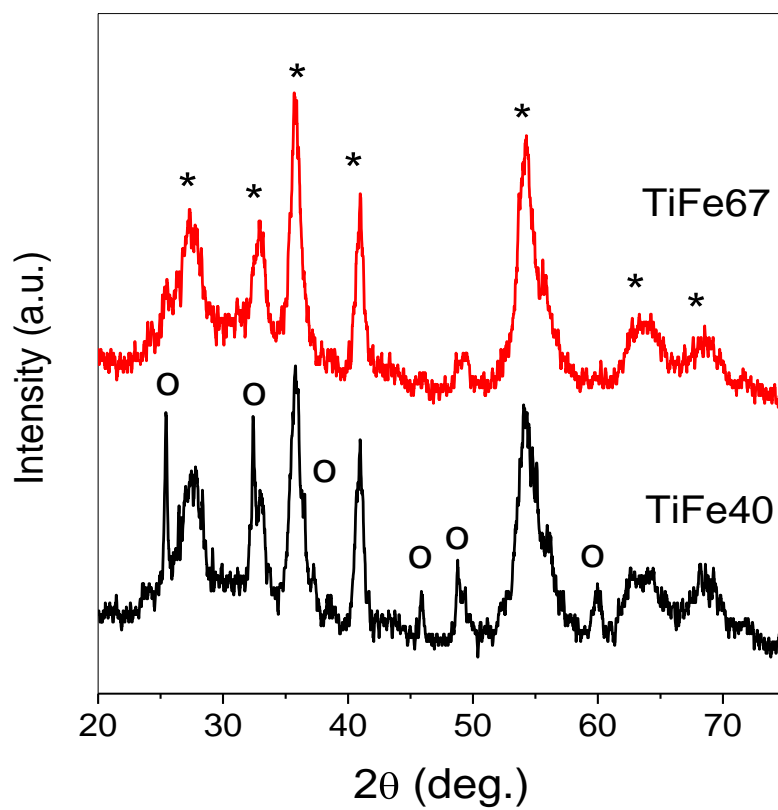
Figure 2.9: XRD patterns of TiFe40 and TiFe67 at 600 °C. o: pseudobrookite, *: pseudorutile
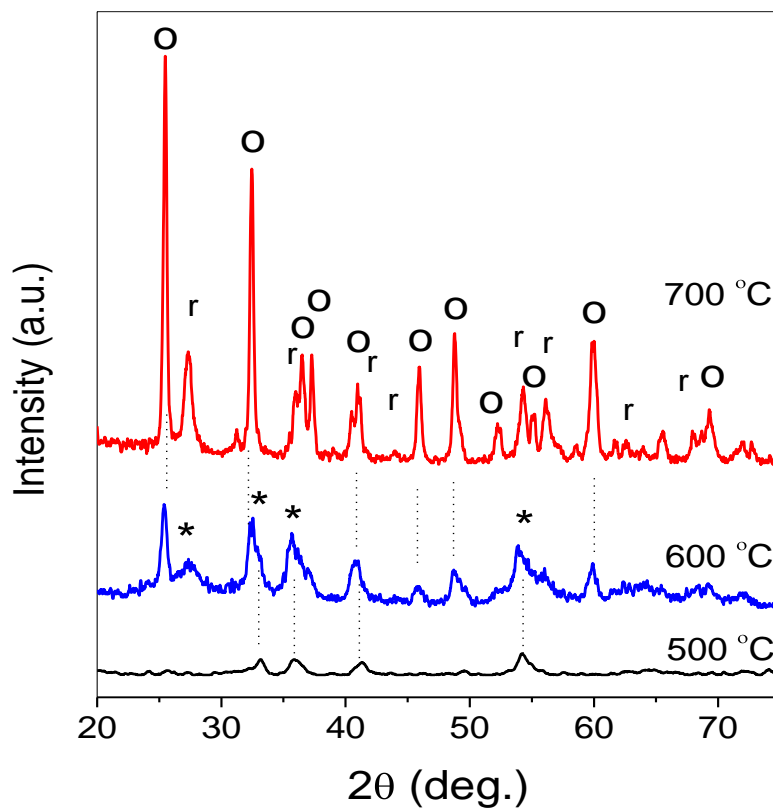
Figure 2.10: XRD patterns of TiFe50 after calcination at different temperatures. o: pseudobrookite, r: rutile, *: pseudorutile

Table 2.4: Summary of the structures detected by XRD after calcinations at 500-700 °C

Composite	Calcination Temperature (°C)		
	500	600	700
TiO_2	Anatase, rutile	Anatase, rutile	Anatase, rutile
TiFe5	Anatase	Anatase	Anatase, rutile
TiFe10	Anatase	Anatase	Anatase, rutile
TiFe15	Anatase, Pr	Anatase, Pr	Rutile, Pb
TiFe20	Anatase, Pr	Anatase, Pr	Pb, rutile
TiFe40	Amorphous, Pr	Pb, Pr	Pb, rutile
TiFe50	Amorphous, Pr	Pb, Pr	Pb, rutile
TiFe67	Amorphous	Pr, Pb	Pb, rutile, α-Fe_2O_3

The main conclusions from the results described above can be summarized as follows: (1) Regardless of the iron concentration, Pr formation is a favored initial binary oxide product and seems to be the dominant phase at 500 °C, but eventually decomposes to Pb and rutile upon calcination at 700 °C. (2) The absence of evidence for segregated irons oxides in TiFe40 at all temperatures indicates that pure Pr phase formed first, at 500 °C, which means that the

preparation of a pure Pr phase is possible under the employed conditions with calcination at temperatures as high as 500 °C. (3) A composite containing equal concentrations of both metal ions result in a mixture of only Pr and Pb at 600 °C. (4) The presence of high concentration of iron ions, such as in the case of TiFe67, resulted in the formation of little segregated α-Fe_2O_3, on the account of the formation of a binary oxide phase, which may explain the relatively higher concentration of rutile at 700 °C in TiFe67. This also means that pure Pb is not possible under the current preparative conditions and further tuning of the experimental conditions might be needed.

2.3.4 DRIFT Study

Selected composites were characterized by DRIFTS. Figure 2.11 shows the spectra of uncalcined TiFe10 recorded at temperatures between 150-500 ^{0}C under the flow of nitrogen. The spectral regions of 400-1000 cm^{-1}, where absorptions due to metal-oxygen (M-O) stretching vibration typically appear, and the region of 2600-4000 cm^{-1}, where C-H and O-H absorptions (ν_{O-H} and ν_{C-H}) take place, are presented. It was noticed that peaks due to bulk OH and adsorbed water in the region 3000-3600 cm^{-1}, and the associated O-H bending modes around 1650 cm^{-1}, as well as ν_{C-H} from organic residues, 2850-3000 cm^{-1}, disappeared almost completely in the temperature range of 350-450 ^{0}C. Meanwhile, a new OH peak around 3700 cm^{-1} evolved and was, to some extent, retained at elevated temperatures, 450-500 ^{0}C. Figure 2.12 shows the spectra of calcined TiFe10 and TiFe40 compared with those of the single metal oxides recorded at 400 ^{o}C. Although the peaks in the 400-1000 cm^{-1} region are very broad and largely

overlap, making their interpretation difficult, the enhanced absorptions below 600 cm^{-1} and around 800 cm^{-1} clearly indicate significant changes in the M-O bonding, which may indicate the formation of Ti-O-Fe hetero-linkage. One observation that is noteworthy is the noticeable absorptions below 500 cm^{-1} in the spectrum of TiFe40 which indicates relatively weaker M-O bonds. In addition, the new peaks around 3700 cm^{-1} and 1400-1500 cm^{-1} in the spectrum of TiFe10 indicate the formation of new strongly bound isolated OH groups on the surface that don't exist in TiO_2. The formation of the new stable OH groups can be referred to the need for charge balance due to the difference between the valences of both metal ions in the lattice, where the iron ions substitute the titanium ions [58]. The fact that these features appear in the TiFe10 and do not appear in TiFe40 support this explanation since TiFe40 is composed mainly of a binary oxide phase where the stoichiometry allows for charge balance. The presence of such OH groups are very often important in heterogeneous catalysis where they may act, in some reactions, as surface active sites and may promote catalytic reactions. In conclusion, the DRIFT study showed changes in the M-O bonding that confirmthe formation of Ti-O-Fe linkage, and new stable OH groups in TiFe10 compared with pure TiO_2.
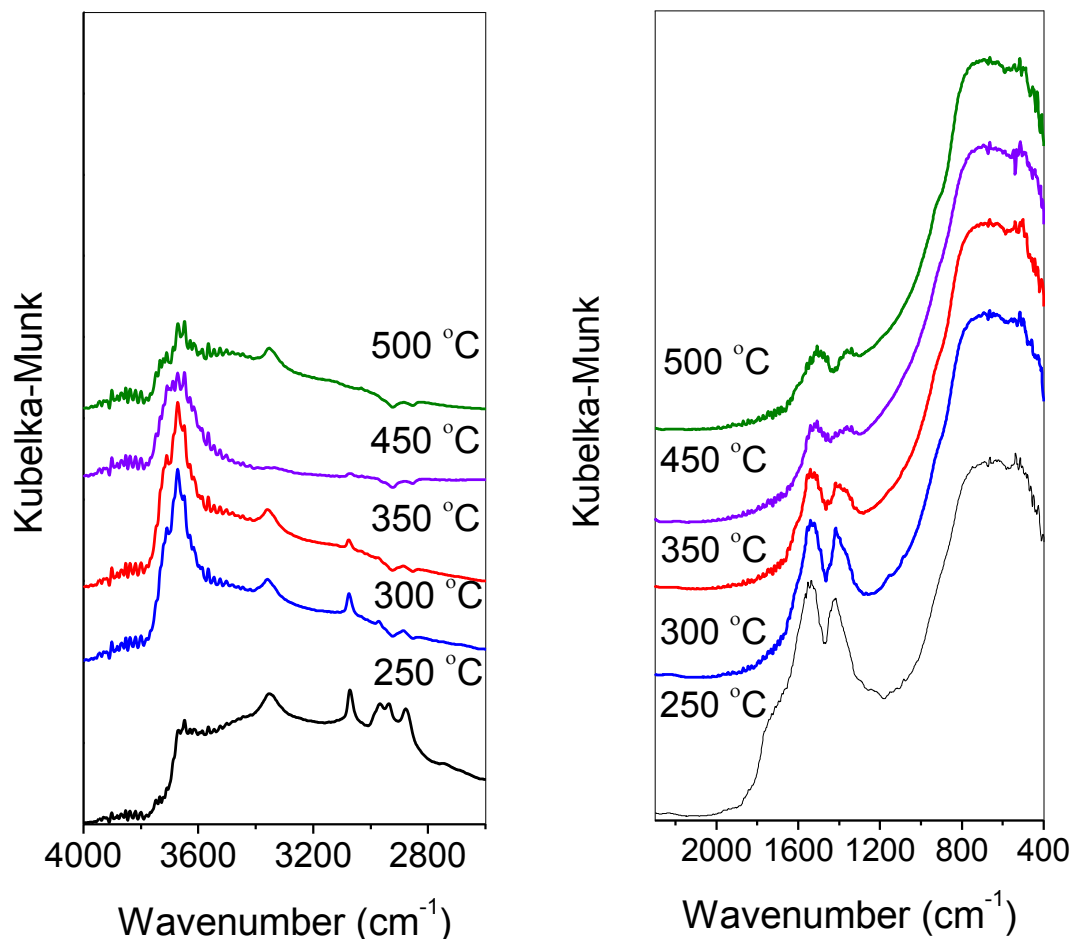
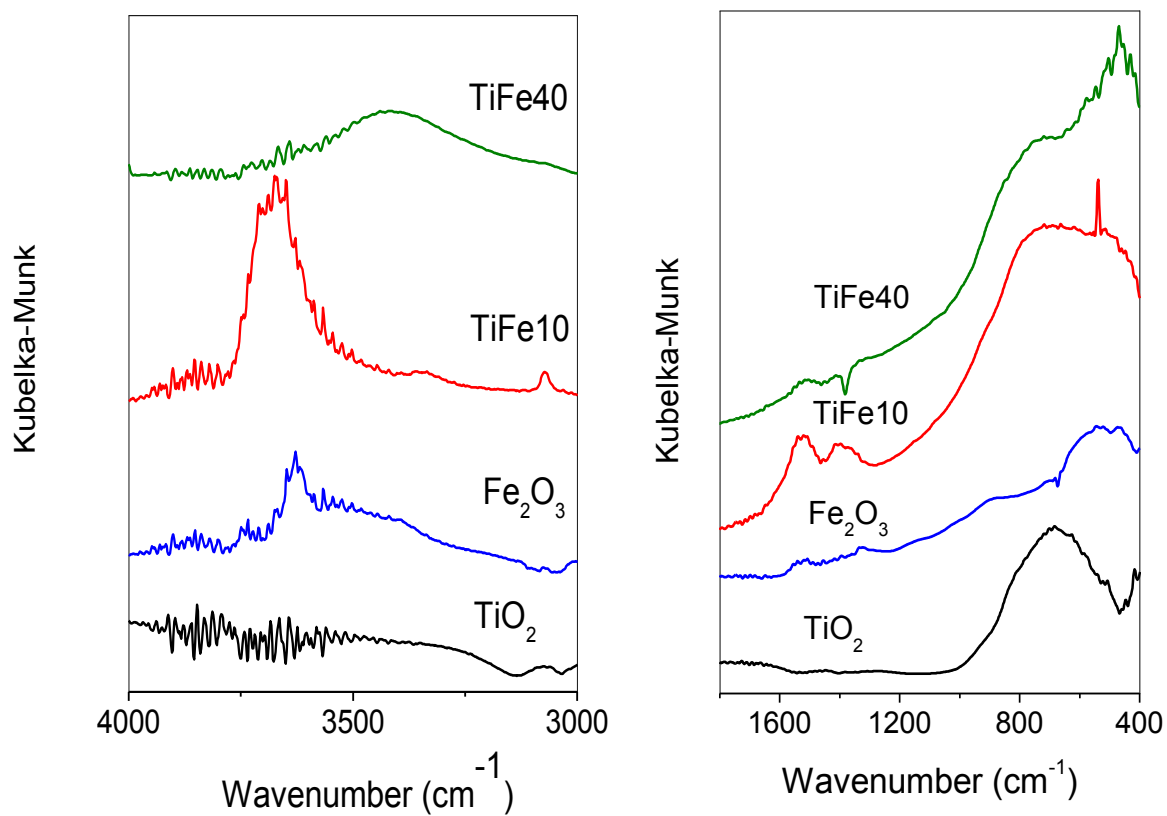Figure 2.11: DRIFTS of TiFe10 during calcination at different temperatures

Figure 2.12: DRIFTS of TiFe10 and TiFe40 compared with single metal oxides at 400 °C

2.3.5   Surface Area and Porosity

Xerogel and aerogel mixed oxides possessed significantly higher surface areas than their parent single metal oxides, and the surface area increased as the Fe(III) concentration increased as shown in Table 2.5 for all xerogel samples. This increase can be referred to two reasons. First, the well dispersion of the iron ions which hinders the segregation of a pure single-metal oxide phase and hence the crystal growth. Second, the enhanced gel formation in the presence of iron ions further enhanced the surface area as well known for sol-gel prepared powders. The composites with high (40-67%) iron concentration possessed significantly higher surface areas than many analogous titania-based or iron oxide-based materials reported in the literature. Besides their high surface areas, these xerogel composites showed relatively high total pore volumes and sharp pore size distributions with pore diameters in the range of 3-6 nm as shown in Table 2.5.

The N_2 adsorption-desorption isotherms for all composites were of H4-type (IUPAC classification) with well-defined hysteresis loops that are characteristics of mesoporous powders as shown in Figure 2.13. The plateau at $P/P_o > 0.8$ indicates the absence of macropores, which is also indicated in the pore size distribution plots shown in Figure 2.14, where narrow pore size distributions are observed for all composites. Although TiO_2 showed a small hysteresis loop for mesopores, the total pores is very small compared with the composites. On the other hand, the loop of Fe_2O_3 isotherm is shifted to a higher range of relative pressure indicating large range of mesopores and macropores as also indicated by it pore size distribution in Figure 2.14a. While all pores in the composites are less than 10 nm, there is zero porosity in Fe_2O_3 in the range below 17 nm. In addition,

its small amount of pores are distributed over a very wide size range. The
observed textural properties of iron oxide is usually what is observed for very
crystalline solids with large crystal size which is also supported by the calculated
crystal size based on the XRD results above. Although all composites exhibited
modified textural properties compared with single-metal oxide, composites with
40 and 67% iron are particularly interesting as they possess significantly high
surface area, high porosity, and sharp pore size distribution of mesopores.

Table 2.5: Surface area and pore characteristics of xerogel samples prepared in the
presence of PO

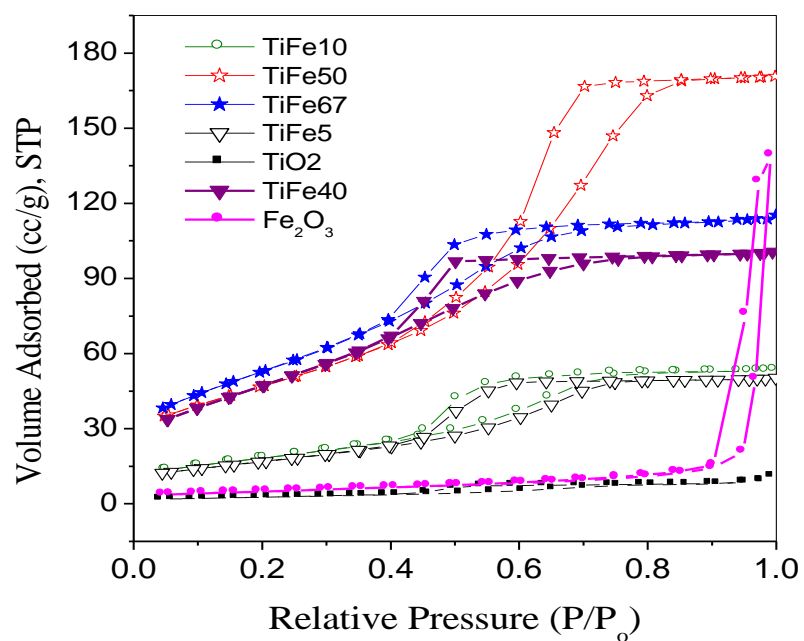| Composition	S_{BET} (m^2/g)	Pore volume (cc/g)	Pore size (nm)
TiO_2	10	0.01	5.8
α-Fe_2O_3	18	0.08	17.3
TiFe5	61	0.08	5.0
TiFe10	66	0.09	5.0
TiFe40	178	0.16	3.5
TiFe50	194	0.27	6.2
TiFe67	217	0.18	3.6

Figure 2.13: N$_2$ adsorption-desorption isotherms of xerogel composites
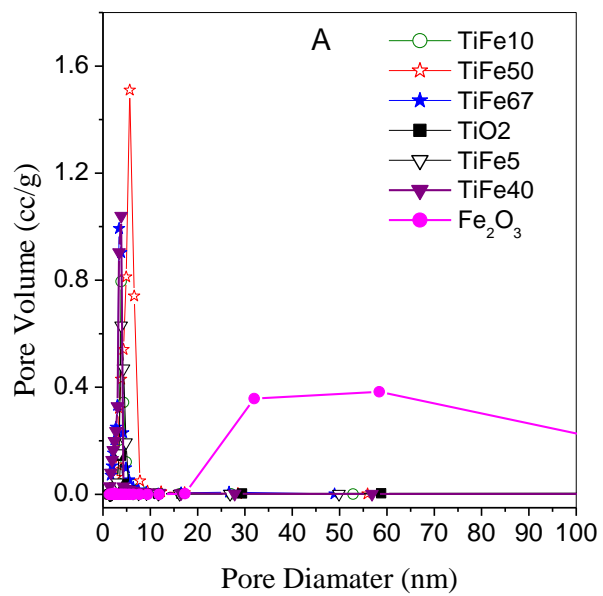
Figure 2.14a: Pore size distribution of xerogel composites in the range 1-100 nm
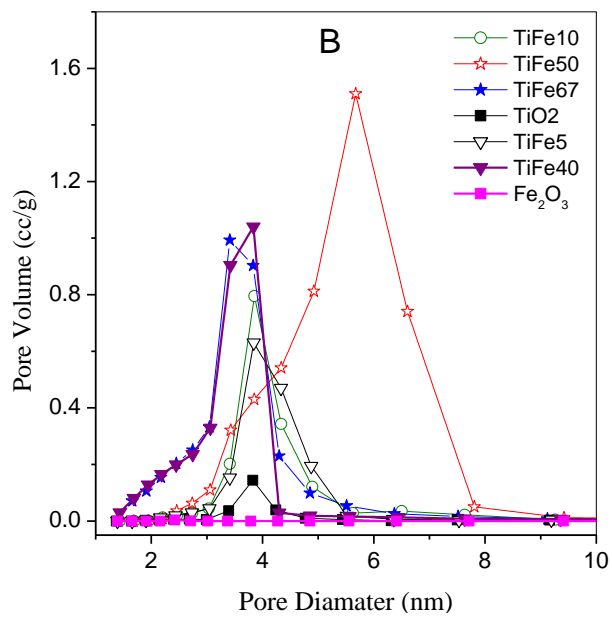
Figure 2.14b: Pore size distribution of xerogel composites in the range 1-10 nm

2.3.6 The Effect of Propylene Oxide on Textural Properties

The presence of PO was found to have a significant effect on the structure of the product in the case of pure iron oxide where it favored the formation of maghemite over hematite which was usually the product in its absence. This observation was not investigated further in this work and is the subject of another ongoing research on pure iron oxides and Ti-modified iron oxides. In the case of composites in the present study, the presence of PO was also found to affect the structure of the final but to a lesser extent than in the case of pure iron oxides. It generally enhanced the formation of Pr as shown for the case of TiFe20 in Figure 2.15. For composites with lower iron content, 5 and 10%, no effect was observed since iron ions were mainly dispersed in the titania lattice. In addition, it was noticed that it enhanced the amorphous nature of composites with high iron content such as in TiFe67 and resulted in segregation of hematite as shown in Figure 2.16. The effect of PO was also studied for TiFe40 at different calcination temperatures and no significant effect on the structure of the product was observed.
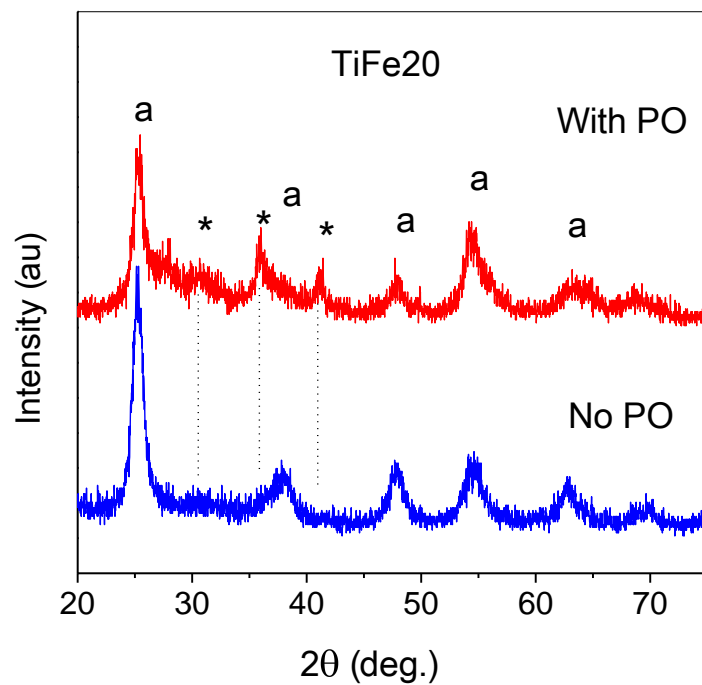
Figure 2.15: XRD patterns of TiFe20 prepared in the presence and in the absence of PO. a: anatase, *: pseudorutile
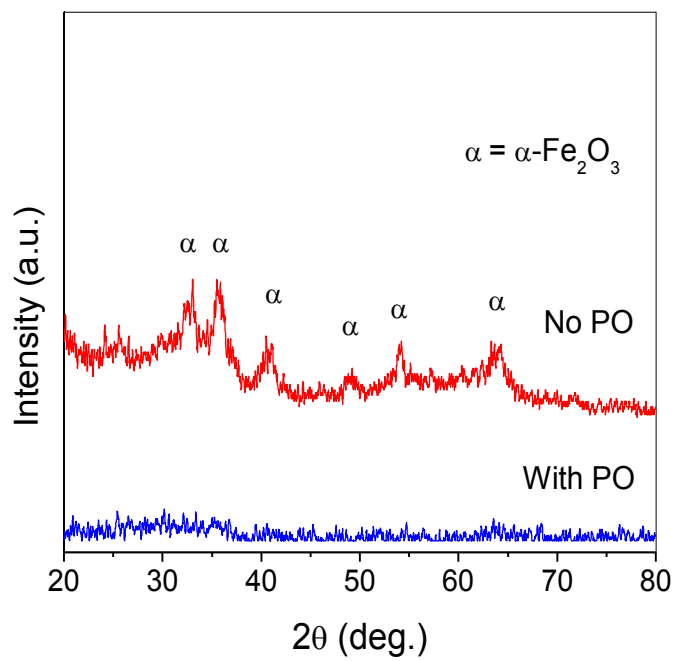
Figure 2.16: XRD patterns of TiFe67 prepared in the presence and in the absence of PO

The effect of PO on the textural properties was studied for selected composites that were prepared in its presence as well as in its absence as shown in Table 2.6. Although it generally enhanced the gel formation as discussed above, the surface area and porosity were not significantly affected by its presence in the studied composites as shown in Table 2.5 and Figures 2.17 and 2.18 which present the N_2 sorption isotherms and pore size distributions of the composites studied in the presence as well as in the absence of PO. All isotherms show hysteresis loops that reflect the dominance of mesopores as also shown by the pore size distribution plots. It should be also noted that the role of PO was found to depend on the solvent and the precursor employed which was not investigated further in this study. These results may indicate that there might be no need to use PO as a gelation promotor in the preparation of iron titanates since gel formed in its absence and it had no significant effect on the textural properties.

Table 2.6: Surface area and pore characteristics of xerogel products prepared in the presence and in the absence of PO

M^{n+}	PO	S_{BET} (m^2/g)	Pore volume (cc/g)	Pore size (nm)
TiFe5	yes	61	0.08	5.0
TiFe5	No	82	0.08	4.0
TiFe67	yes	217	0.18	3.6
TiFe67	No	168	0.20	4.9
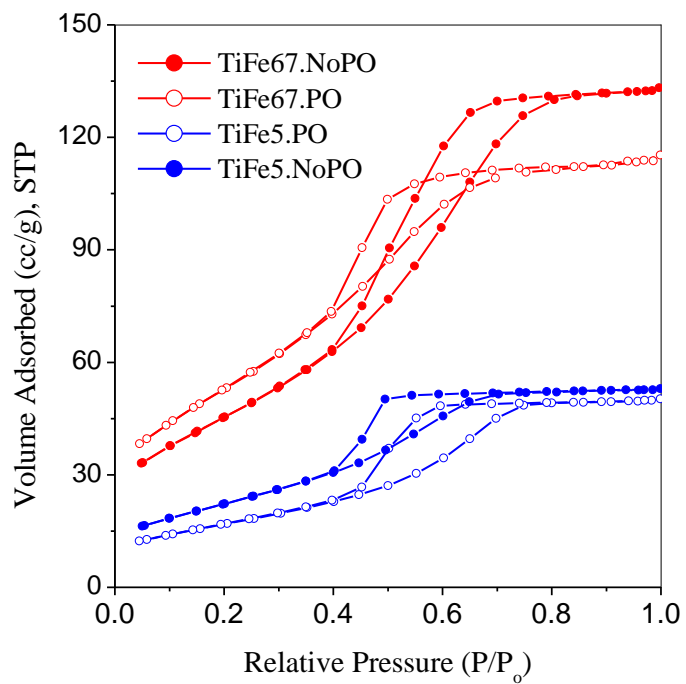
Figure 2.17: N_2 adsorption-desorption isotherms of xerogel powders prepared in the presence and in the absence of PO
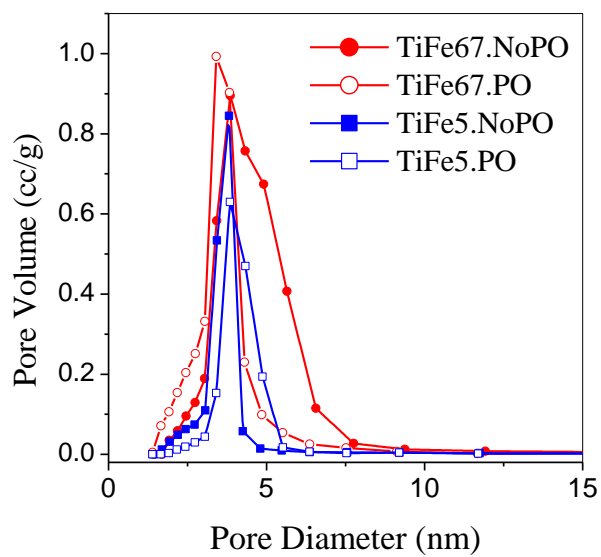
Figure 2.18: BJH pore size distribution of xerogel products prepared in the presence and in the absence of PO

2.3.7   Aerogel vs. Xerogel Products

Aerogels were also prepared for selected composites by removing the solvent from the gels under the solvent (2-propanol) supercritical conditions. The aerogel processing does not seem to affect the structure of the composites. However, the supercritical conditions employed resulted in slightly enhanced crystallinity.

As shown in Table 2.7, the aerogel products after calcination possessed significantly high surface areas and total pore volumes compared with their xerogel counterparts. It is noticed that the pores in the aerogel are larger in size and have wider distribution compared with xerogel product as shown in Figures 2.19-2.22. Hysteresis loops at higher relative pressure (P/P_o) indicate large pore diameters. This can be referred to the fact that the particles are more packed in the xerogel compared with aerogel products where the particles are loosely packed resulting in larger inter-particle pores. However, the pores in the aerogels are all in the mesoporic range as shown in Figure 2.21. In addition, the porosity also depends on the composition, where larger iron concentration was associated with large pore volume and pore diameter.

Table 2.7: Surface area and pore characteristics of selected xerogel products
compared with their aerogel counterparts

M^{n+}	PO	S_{BET} (m^2/g)	Pore volume (cc/g)	Pore size (nm)
TiFe10	yes	66	0.09	5.0
TiFe10-a	yes	117	0.26	8.2
TiFe67	No	168	0.21	4.9
TiFe67-a	No	173	0.79	18.3

Figure 2.19: N_2 adsorption-desorption isotherms of TiFe10 aerogel vs. xerogel prepared in the presence of PO

Figure 2.20: Pore size distribution of aerogel vs. xerogel TiFe10 prepared in the presence of PO

Figure 2.21: N_2 adsorption-desorption isotherms of calcined aerogel vs. xerogel
TiFe67 prepared in the absence of PO

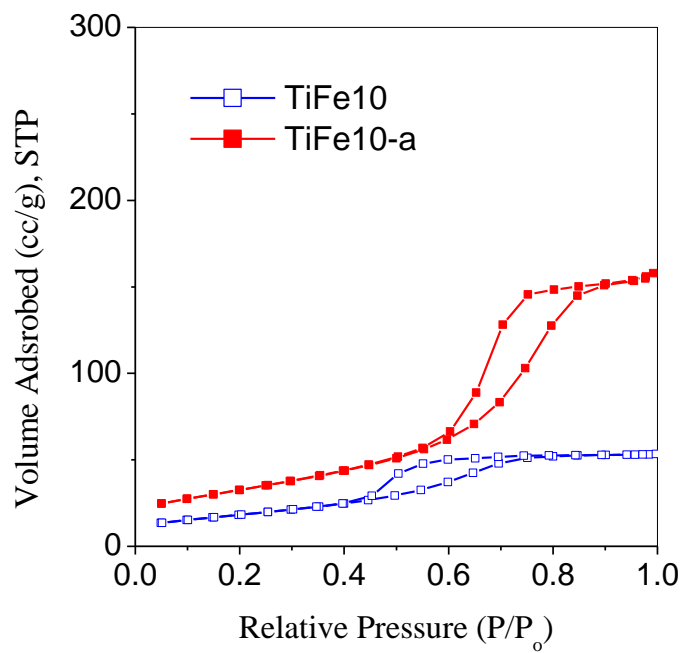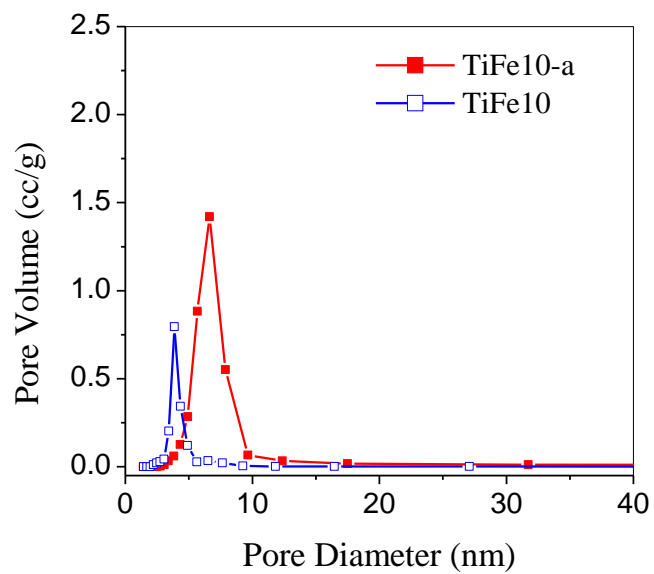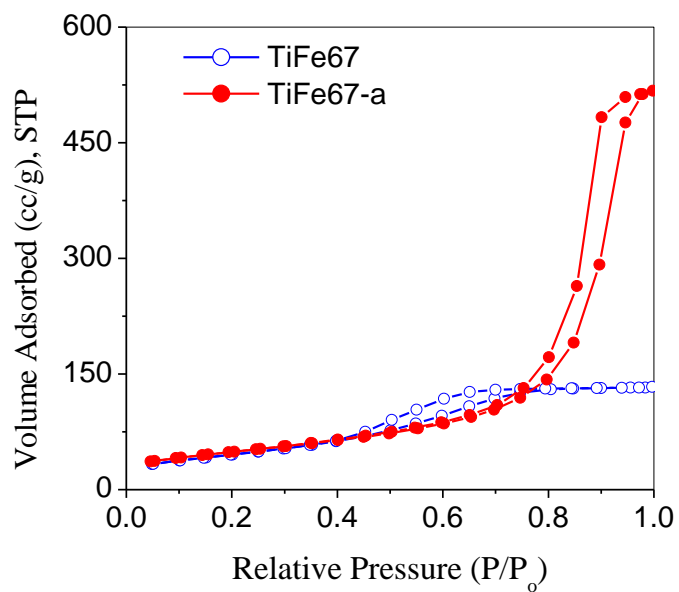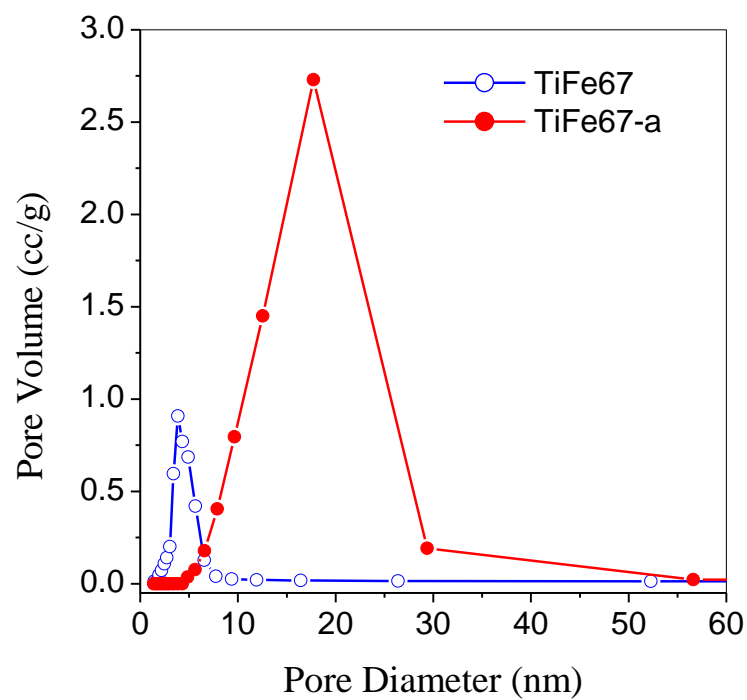Figure 2.22: Pore size distribution of aerogel vs. xerogel TiFe67 prepared in the absence of PO

2.3.8   H$_2$-Temperature Programing Reduction Studies

The TPR profiles of single metal oxides and mixed oxides are shown in Figure 2.23. The profile of α-Fe$_2$O$_3$ showed reduction in two temperature regions, 380-550 ^{0}C and >650 ^{o}C centering around 900 ^{0}C. The peak in the temperature range of 380-550 ^{o}C can be referred to first, partial reduction of Fe(III) ions to Fe(II) forming Fe$_3$O$_4$ and then to further reduction forming FeO. The broad peak around 900 ^{o}C can be referred to even further reduction of Fe(II) to zero-valent iron atoms. Interestingly, the profiles of the composite oxides indicate that the reducibility depends significantly on the composition. First, the reduction peak in the high-temperature range disappeared completely in the profiles of composites with Fe(III) $\leq$ 20%, which may indicate that only reduction of Fe$_2$O$_3$ to Fe$_3$O$_4$ and to FeO takes place in these composites. This behavior can be correlated with the fact that Fe(III) ions in composites with low iron content are well dispersed.

In the profiles of TiFe50 and TiFe67, only a small peak appears at temperatures <700 ^{o}C which still indicates that the lower temperature reduction dominates. The amounts of hydrogen consumption are shown in Table 2.8, where the results clearly indicate an enhanced reducibility of the composites compared with the single metal oxides, which indicates a weaker Fe-O bonding in the mixed oxides. These results are in agreement with the DRIFTS results where absorptions at lower values of wavenumber were observed for the binary oxide phases indicating weaker M-O bonds. The enhanced reducibility would be more pronounced if the results were reported per mol of Fe(III) present in the composites since TiO$_2$ is not noticeably reducible.

Table 2.8: Hydrogen consumption in the H_2-TPR of the composites and the parent single metal oxides

Composition	Temperature (°C)	H_2 (μmol g^{-1})	Temp. (°C)	H_2 (μmol g^{-1})	Total H_2* (μmol g^{-1})
TiO$_2$	-	0	-	0	0
α-Fe$_2$O$_3$	429	175	491	1068	1243
TiFe10-x	394	18	468	271	289
TiFe10-a	390	21	446	196	217
TiFe20	410	72	488	521	593
TiFe50	430	254	508	1388	1642
TiFe67	427	263	512	1344	1641
	346	34			

*The total refers to total reduction at temperatures below 600 ^{0}C.
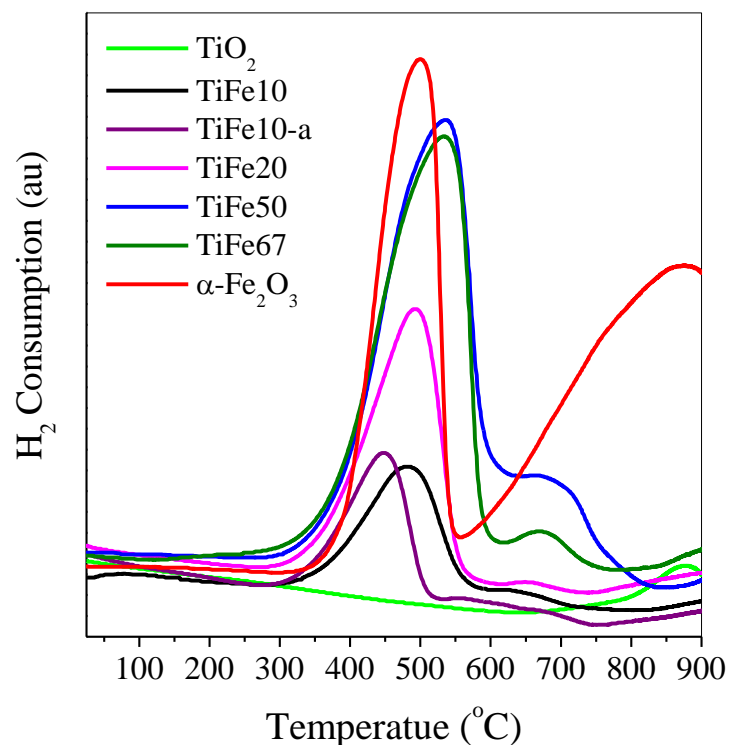
Figure 2.23: H_2-TPR profiles of the mixed oxide composites, TiO_2, and α-Fe_2O_3

2.4 Conclusions

The products that form from titania modified with different concentrations of Fe(III) ions and phase transformations during the preparation of iron titanates was investigated. The textural properties including surface area and porosity were studied. Since the prepared compounds will be tested as oxidation catalysts, their reducibility was also investigated. In addition, the effect of the presence of propylene oxide on the structure and the textural properties of the products was studied.

The presence of PO as well as the presence of hetero-ions was found to play a key role in promoting gel formation at certain concentrations. However, the role of PO was affected by the presence of excess water in the solution. While in the presence of a single metal ions colloidal solutions and very fine precipitates were obtained, gels formed readily from mixed solutions containing 5-15% Fe (III) in the presence of PO. On the other hand, concentrations of Fe(III) of 20%, under the same conditions, resulted in some precipitation. When iron content was increased to concentrations between 40 and 66.7%, gels formed readily even in the absence of PO.

It was found that Fe(III) concentration as high as 10% can be well dispersed in the titania lattice before binary oxide phases can form. Moreover, iron concentration lower than 10% can be used to enhance the stability of the anatase phase. However, Fe(III) higher than 10% resulted in the formation of anatase and Pr, initially, which converted to rutile and Pb upon heating at elevated temperatures. Regardless of the iron concentration, Pr formation was a favored

initial binary oxide product and was the dominant phase at 500 °C, which decomposed to Pb and rutile upon calcination at 700 °C.

It was concluded that the preparation of a pure Pr phase is possible under the employed preparative conditions starting with the appropriate amounts of both metal precursors and with calcination of the final product at temperatures as high as 500 °C. However, the presence of high concentration of iron ions, in the case of TiFe67, resulted in the formation of little segregated α-Fe_2O_3, on the account of the formation of a binary oxide phase. This means that pure Pb is not possible under the current preparative conditions and further tuning of the experimental conditions might be needed.

Xerogel and aerogel mixed oxides possessed significantly higher surface areas than their parent single metal oxides, and the surface area increased as the Fe(III) concentration increased. Furthermore, the TPR results indicated an enhanced reducibility of the composites, which indicates a weaker Fe-O bond in the mixed oxides and hence, a more labile lattice oxygen, which may lead to enhanced catalytic oxidation.

Chapter 3: Catalytic Oxidative Degradation of Toluene

3. 1 Introduction

Volatile organic compounds (VOCs) are main contributors to environmental pollution and are emitted in the environment from different sources including industries and fossil fuel combustion. They present a serious direct threat to the human health and to the environment [59-61]. Therefore, control on emission of VOCs as well as developing technologies for their removal has been of great importance and a global concern. While different technologies have been investigated and developed for VOCs removal including adsorption, biodegradation, and thermal incineration, catalytic combustion has been found to be a promising effective remedy for their emission control and removal [62-67].

Catalytic combustion of VOCs has been investigated over a wide variety of catalysts including metal particles and metal oxide systems. While several metal-based catalysts have shown promising catalytic activities, metal oxide catalysts offer some advantages including cost-efficiency and thermal textural stability. Catalysts based on transition metal oxides, especially those involve oxides of V, Mn, Cr, Fe, Ce, Cu, and some others are commonly investigated and employed as oxidation catalysts [61-64,66,67]. Catalysts based on iron oxides have shown promising catalytic activity in the oxidative decomposition of different VOCs and have attracted special attention due to their cost-effective preparation and their availability [68,69]. One of the limitations associated with the use of many transition metal oxides, including iron oxides, is their low stability against sintering when employed at high temperatures and therefore, rapid considerable decrease in their catalytic activity. It has been found that catalyst based on doped

or bulk mixed oxides offer several advantages including textural modification exhibiting improved resistance to sintering and enhanced porosity [70]. Stability against sintering preserves higher surface areas and enhanced porosity improves diffusion of molecules through the catalyst. In addition, the presence of more than one metal ion in the oxide matrix may offer other advantages including structural and electronic modification by stabilizing a particular phase, as an example, and playing synergic roles in the oxidation reduction process [70].

Titanium-iron oxides have shown improved performance in in various application including semiconductors, ferromagnetic materials, ceramics, and catalysis [71-73]. They include a variety of binary oxides including ilmenite ($FeTiO_3$), pseudobrookite (Fe_2TiO_5), and pseudorutile ($Fe_2Ti_3O_9$) [74-76]. The preparation of pure single phases of Fe(III)-based compounds is a challenge due to easy segregation of single-metal oxide phases and structure instability at elevated temperatures.

Fe(III)-modified titania and Fe(III)-Ti(IV) binary oxides as possible oxidation catalysts have received much less attention as possible catalysts compared with their single-metal oxides. In addition, the effect of different preparative conditions on the structures that may evolve from sol-gel preparation of these materials and the effect of this composition on their catalytic activity have never been reported. In this chapter, the results of a study on the catalytic activity of the prepared Fe(III)-modified titania and Fe(III) titanates in the oxidation of toluene are discussed.

3.2 Experimental Procedure

The catalytic activity of the prepared catalysts was studied on a solid-vapor reaction setup with a U-shaped stainless steel fixed bed reactor of 4mm internal diameter as shown in Figure 3.1 and Figure 3.2. The reaction temperature was monitored using an electrical furnace and a K-type thermocouple positioned at the middle of the catalyst bed. In each experiment, 0.15 g of the catalyst powder, 350-500 mesh size, was packed in the reaction tube between a stainless steel frit and a glass wool plug. Toluene was introduced using a saturator at 21 °C and the reaction mixture consisted of 1100 ppm, 4% or 16% air, and He balance with a total flow rate of 50 mL/min. Flow rates were monitored by mass flow controllers from Alicat Scientific.

All tested catalysts were already calcined at 400 °C for 3 hours, and before each reaction they were treated at 350 °C for 1 hour under air with a flow rate of 25 mL/min. The composition before and after reaction was analyzed using an on-line gas chromatograph (GC-2010, Shimadzu) equipped with a Barrier Ionization Discharge (BID) detector capable of detecting inorganic gases as well as hydrocarbons. The transfer line between the toluene saturator and the GC was heated at 150 °C. The concentrations before the reaction were measured using a bypass line and the conversion was calculated based on the difference between the inlet and outlet concentrations. In the light-off experiments, each reaction temperature was held for 15 minutes before sampling of the products which was done twice over a period of 45 minutes and the average concentration of both measurements was considered in the calculations of the conversion and yields. The catalytic activity was studied for the composites TiFe10 and TiFe67 as well as for the single-metal oxides TiO_2 and Fe_2O_3 for comparison.

1: Mass flow controllers
2: Toluene saturator
3: Reactor/Catalyst
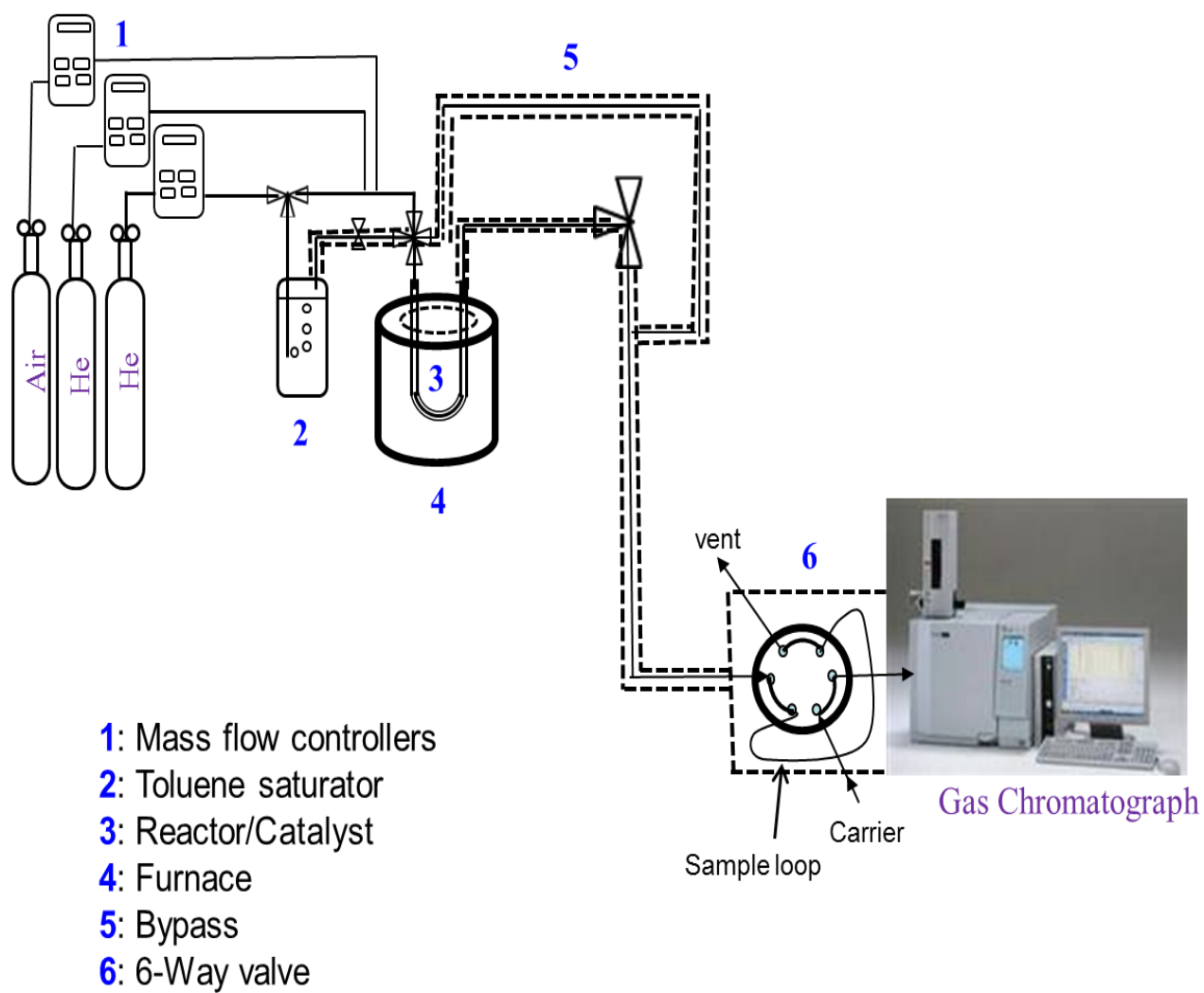**4**: Furnace
5: Bypass
6: 6-Way valve

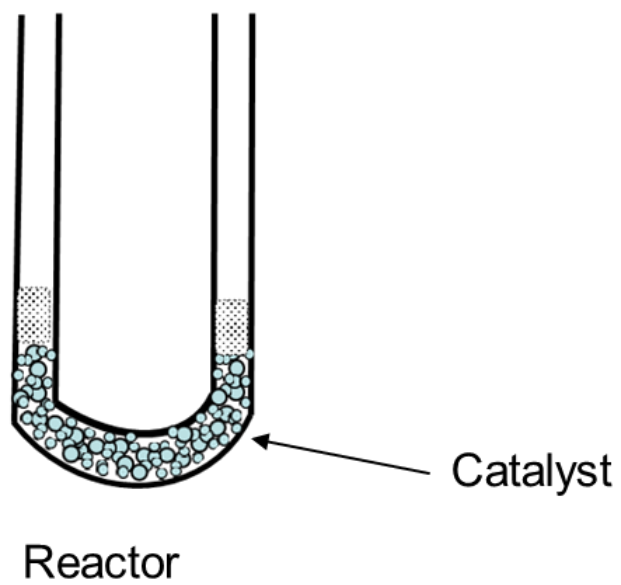Figure 3.1: Reaction Setup used in the catalytic activity study

Figure 3.2: Schematic representation of the reactor and the catalyst bed

3.3 Results and Discussion

3.3.1 Catalysts Reducibility and Textural Characterization

The structural and textural characterization of the prepared catalysts were discussed in chapter 2. Meanwhile, the reducibility and textural properties of the catalysts selected for catalytic studies are compared in this chapter for better correlation between these properties and the catalytic activity.

Compared to the single-metal oxides, the mixed oxide catalysts possessed significantly higher surface areas and total pore volume as presented in Table 3.1. The N_2 adsorption-desorption isotherms of the mixed oxides, shown in Figure 3.3, were of H4-type (IUPAC classification) with well-defined hysteresis loops indicating the formation of mesoporous powders as also indicated by the pore size distribution plots shown in Figure 3.4, where narrow pore size distributions are observed for the mixed oxides.

Although TiO_2 showed a small hysteresis loop for mesopores, the total pores is very small compared with the mixed oxides. On the other hand, the loop of Fe_2O_3 isotherm is shifted to a higher range of relative pressure indicating large range of mesopores and macropores. Besides their high surface areas, the mixed oxide powders showed relatively high total pore volumes and sharp pore size distributions with pore diameters 3.6 and 5.0 nm as shown in Table 3.1. The modified textural properties can be referred to two reasons. First, the well dispersion of the iron ions which hinders the segregation of pure single-metal oxide phases and hence hinders crystal growth. Second, the enhanced gel formation in the presence of both metal ions.

Table 3.1: Surface area and pore characteristics of the mixed Ti-Fe oxide catalysts and the single metal oxides

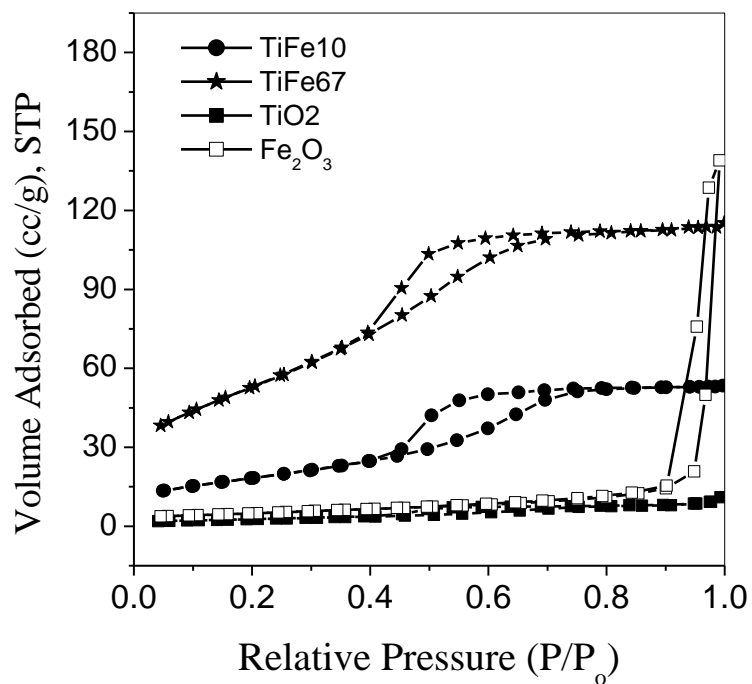| Composition	S_{BET} (m^2/g)	Pore volume (cc/g)	Pore size (nm)
TiO$_2$	10	0.01	5.8
α-Fe$_2$O$_3$	18	0.08	17.3
TiFe10	66	0.09	5.0
TiFe67	217	0.18	3.6

Figure 3.3: N$_2$ adsorption-desorption isotherms of the mixed oxides and the single metal oxides
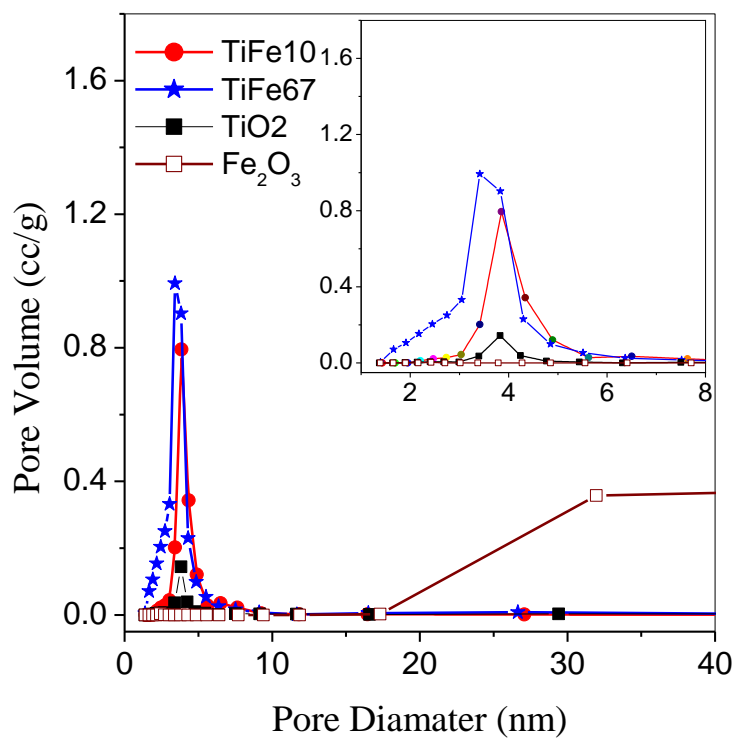
Figure 3.4: BJH Pore size distribution of the mixed oxides and the single metal oxides

The results of the H_2-TPR characterization of the studied catalysts are shown in Table 3.2 and Figure 3.5. The profile of α-Fe_2O_3 showed reduction in two temperature regions, 380-550 ^{0}C and >650 ^{o}C centering around 900 ^{0}C. The peak in the temperature range of 380-550 ^{o}C can be referred to the partial reduction of Fe(III) ions to Fe(II) forming Fe_3O_4 and then to further reduction forming FeO. The broad peak around 900 ^{o}C can be referred to even further reduction of Fe(II) to zero-valent iron atoms. Interestingly, TiFe67 showed a reduction profile that is noticeably different from that of α-Fe_2O_3. First, the reduction peak in the high-temperature range almost completely disappeared. This behavior was also confirmed by observing the same for other related composites such as TiFe50, not shown. Second, the reduction started at slightly lower temperature and extended over a relatively wider temperature range. These observation may indicate that the first reduction step becomes easier and the deep reduction is hindered. Third, TiFe67 showed an enhanced overall reducibility as shown in Table 3.2. The fact that the TiFe67 profile shows reduction at lower temperature than α-Fe_2O_3 and that it extends over a larger temperature range is an indication of the formation of different metal-oxygen bonds including bonds with more labile oxygen atoms. In addition, it shows a larger total H_2 consumption indicating higher overall reducibility than α-Fe_2O_3 as shown in Table 2, which presents the amounts of H_2 consumed in the temperature range of 25-600 °C. The TPR results were supported by the results of the DRIFTS study where absorptions due to metal-oxygen bond vibrations in the mixed oxides were enhanced at lower values of wavenumber, as shown in Figure 3.6, indicating weaker bonds.

Table 3.2: Hydrogen consumption in the H_2-TPR of the mixed and the single metal
oxides in the temperature range of 25-600 °C

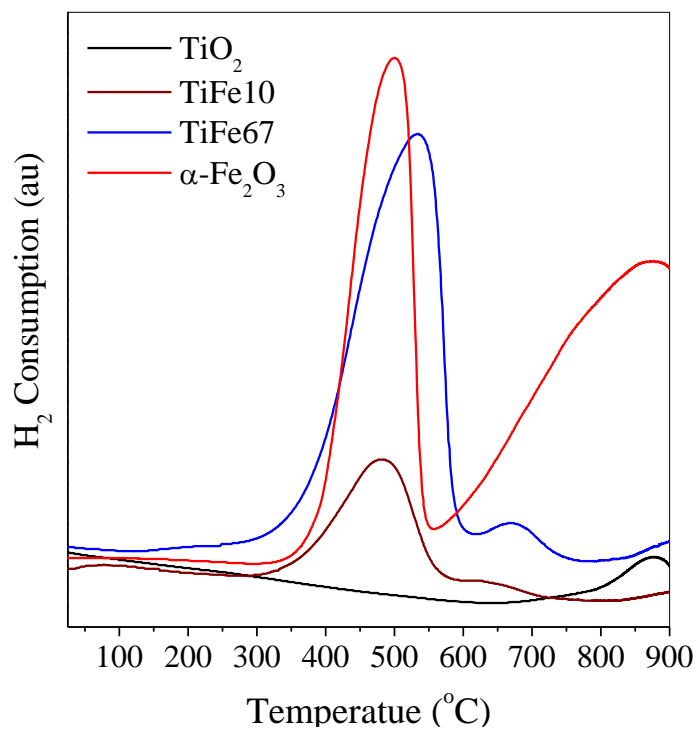| Composition	Temperature (^{0}C)	H_2 (μmol g^{-1})	Temperature (^{0}C)	H_2 (μmol g^{-1})	Total H_2 (μmol g^{-1})
TιO$_2$	-	0	-	0	0
α-Fe$_2$O$_3$	429	175	491	1068	1243
TiFe10	394	18	468	271	289
TiFe67	427	263	512	1344	1641
	346	34			

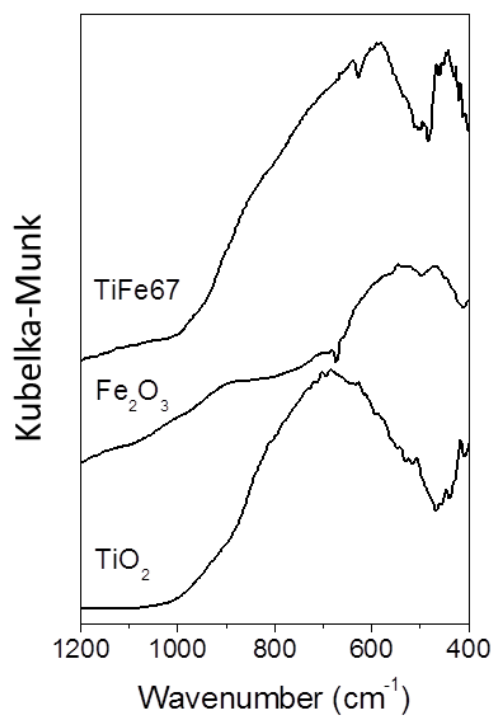Figure 3.5: H₂-TPR profiles of the mixed and the single metal oxides

Figure 3.6: DRIFT of TiFe67 and α-Fe₂O₃.

3.3.2 Catalytic Activity

The catalytic activity of TiFe10, TiFe67, α-Fe$_2$O$_3$, and TiO$_2$ as well as their selectivity to CO$_2$ product were studied at temperatures between 150 and 500 °C. Reactions were tested in the presence of low (4%) and high (16%) air concentrations. While 16% air resulted in the formation of CO$_2$ as the only carbon product, 4% air was associated with the formation of some benzene, beside CO$_2$, at temperatures $\geq$ 350 °C and a carbon balance around 94% was obtained in both cases. The toluene conversion and products yields were calculated as follows:

$$Conversion\ (\%)\ = \frac{[Tol_{in}] - [Tol_{out}]}{[Tol_{in}]} \times 100$$

$$CO_2\ yield\ (\%)\ = \frac{[CO_{2out}]}{7 \times [Tol_{in}]} \times 100$$

$$Benzene\ yield\ (\%)\ \frac{[Benzene_{out}]}{[Tol_{in}]} \times 100$$

Figure 3.7 shows the conversion of toluene over the studied catalysts at different temperatures using 4% oxygen in the feed mixture. It is evident that mixed oxides containing both metal ions possessed significantly improved catalytic activity compared with the single-metal oxides, especially at lower temperatures. While α-Fe$_2$O$_3$ and TiO$_2$ showed almost no conversion at150 °C, TiFe10 and TiFe67 showed conversions close to 10% and 24%, respectively. TiFe67 also showed significantly higher catalytic activity than the other tested catalysts, especially at lower temperatures, 150 and 250 °C. Figure 3.8 presents the toluene conversion vs. time-on-stream at 350 °C showing a decrease in the conversion during the first couple of hours and good stability after that.
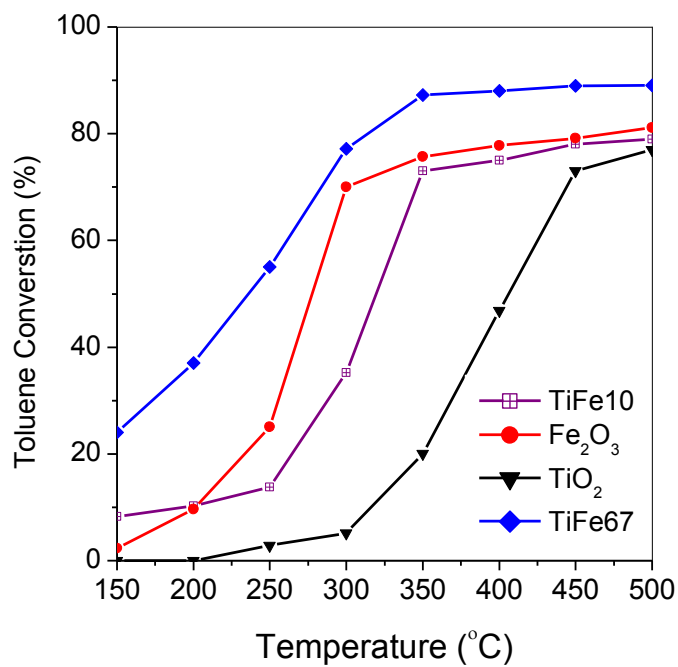
Figure 3.7: Conversion of toluene versus reaction temperature using 4% air in the feed mixture
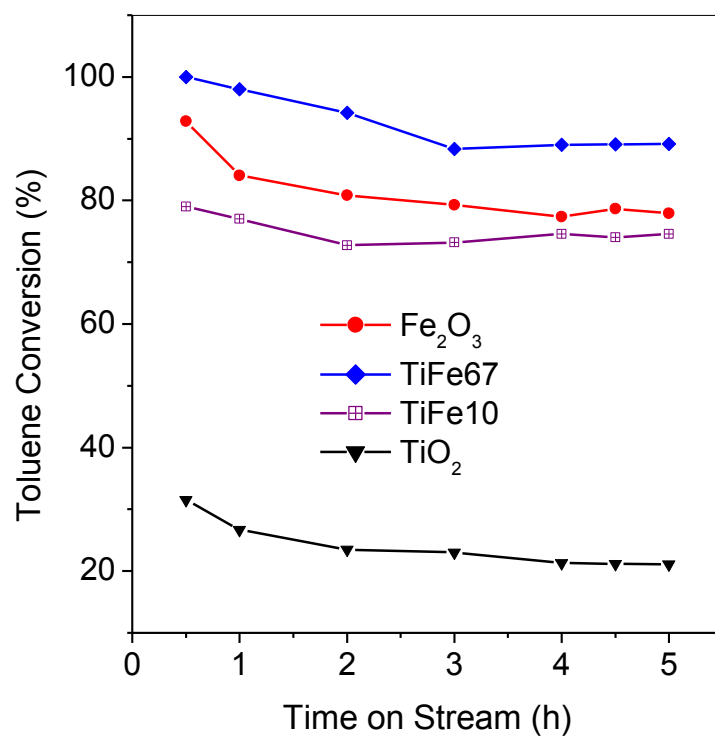
Figure 3.8: Conversion of toluene versus time-on-stream at 350 °C using 4% oxygen in the feed mixture

At temperatures below 300 °C, where the conversion was < 80%, CO_2 was the only carbon product. However at temperatures ≥350 °C, in addition to the main product, CO_2, 2-7% yield of benzene was observed as shown in Figure 3.9. This indicates that under the employed experimental conditions, high conversion is associated with incomplete oxidation resulting in small amounts of benzene. The amounts of benzene were generally larger on the more active catalysts due to the higher conversion. The observation of benzene under low oxygen concentration may indicate that the first step in toluene oxidative decomposition is the cleavage of the ring-methyl bond resulting in an adsorbed benzene ring that undergoes further oxidation to CO_2 in the presence of excess oxygen.
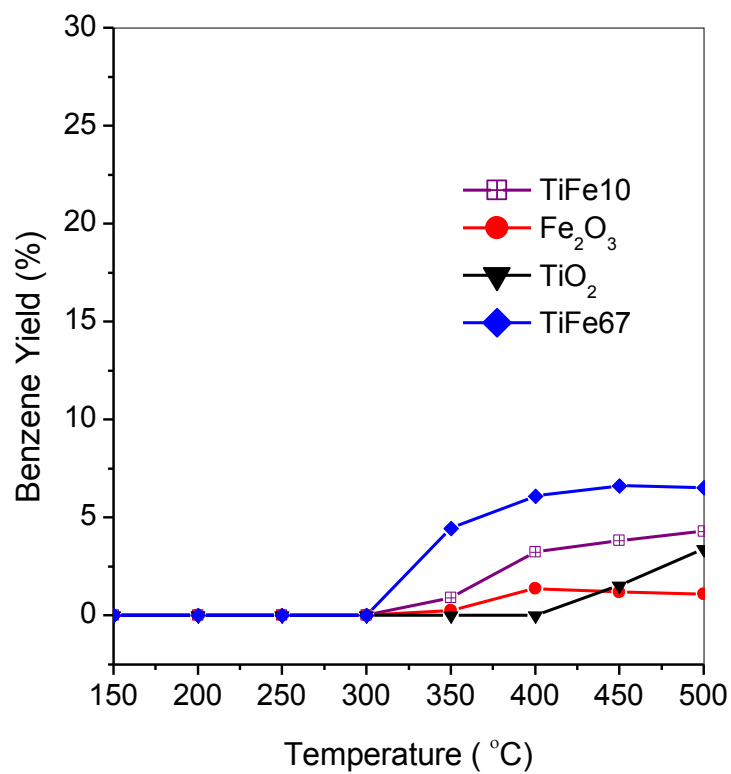
Figure 3.9: Benzene yield at different reaction temperatures using 4% in the feed mixture

Using air concentration of 16% in the gas feed, resulted in complete oxidation of toluene where CO_2 was the only carbon product. Figure 3.10 presents the conversion of toluene at different temperatures and Figure 3.11 shows the CO_2 yield under these conditions. Compared with the other catalysts, FeTi67 resulted in 100% conversion at relatively lower temperature, 300 °C. In addition, it showed significantly higher conversion in the lower temperature range, 150-250 °C, with around 35% conversion at 150 °C. It also showed slightly better selectivity to CO_2 as shown in Figure 3.11. The higher conversion of TiFe67 can be referred, in part, to its significantly higher surface area exposing more coordinately unsaturated active sites. More importantly, the enhanced activity of TiFe67 correlates with its higher reducibility compared with the other catalysts as discussed above.

These results confirm the presence of weaker metal-oxygen bonds as was suggested before based on the TPR and DRIFTS results. Interestingly, the incorporation of 10% Fe(III) ions in the TiO_2 structure significantly increased its catalytic activity to the same level of, and even slightly better than, α-Fe_2O_3. Since the reducibility and the catalytic activity of pure TiO_2 was very low, the significantly enhanced activity upon doping with Fe(III) ions confirms the formation of new metal-oxygen bonds and more labile lattice oxygen atoms. The catalytic activity was also tested on an aerogel TiFe10 (not shown), which possessed significantly high surface area comparable to that of TiFe67, and it showed similar activity to that of xerogel TiFe10. This behavior confirms that the modified catalytic activity is due, mainly, to the structure and the composition rather than to textural properties. Therefore, combining high surface area and significant mesoporosity as well as enhanced reducibility would make TiFe67 a promising oxidation catalyst. In addition, the Ti(IV) ions in the TiFe67 act as

efficient positive centers for initial adsorption through interaction with the ring π-type molecular orbitals. The possible adsorption capability of the Ti(IV) and the redox potential of the Fe(III) ions result in enhanced catalytic activity. For better understanding of the adsorption and reaction pathways, studying adsorbed toluene under different conditions would be an important future work.
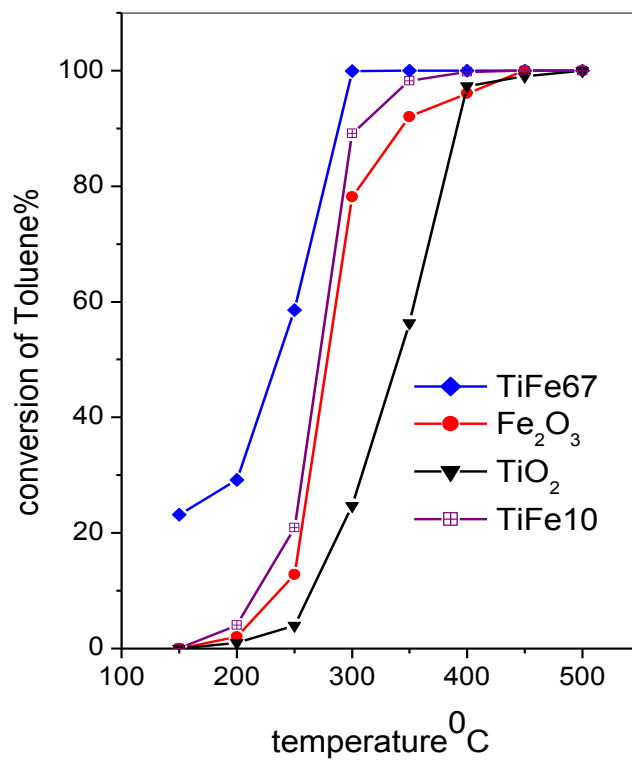
Figure 3.10: Conversion of toluene at different temperatures using 16% oxygen in the feed mixture
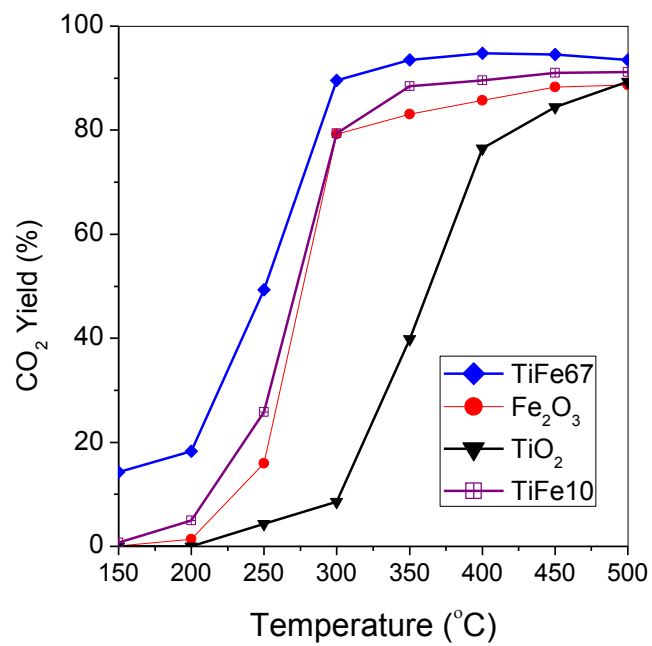
Figure 3.11: CO$_2$ yield at different temperatures using 16% oxygen in the feed mixture

3.4 Conclusions

It was evident that mixed oxides containing both metal ions possessed significantly improved catalytic activity compared with the single-metal oxides, especially at lower temperatures. Using 16% air in the reaction mixture, resulted in deep oxidation to CO_2. On the other hand, lower concentration of air, 4%, resulted in the formation of small amounts of benzene besides the major product CO_2. TiFe67 showed an enhanced catalytic activity making it a promising catalyst for oxidative degradation of VOCs.

Bibliography

[1] Zhang, Xiaodong Zhenping Qu, Xinyong Li, Qidong Zhao, Yi Wang, and Xie Quan."Low temperature CO oxidation over Ag/SBA-15 nanocomposites prepared via in-situ "pH-adjusting" method." *Catalysis Communications* 16.1 (2011): 11-14.

[2] Kum, Jong Min ,Seung Hwa Yoo ,Ghafar Ali ,Sung Oh Cho."Photocatalytic hydrogen production over CuO and TiO_2 nanoparticles mixture." *International Journal of Hydrogen Energy* 38.31 (2013): 13541-13546.

[3] Fechete, Ioana, Ye Wang, and Jacques C. Védrine. "The past, present and future of heterogeneous catalysis." *Catalysis Today* 189.1 (2012): 2-27.

[4] John N. Armor, "A history of industrial catalysis," *Catalysis Today* 163.1 (2011) 3-9.

[5] Julian R.H. Ross. "Chemistry in Two Dimensions," *Heterogeneous Catalysis Fundamentals and Applications*, Elsevier, Oxford, 2012. 1-15.

[6] http://www.nobelprize.org/nobel_prizes/chemistry/laureates/

[7] Bert M. Weckhuysen, Isreal E. Wachs. "Catalysis by Supported Metal Oxides" *Handbook of Surfaces and Interfaces of Materials*, Harcourt USA, 2001. 613 644.

[8] He, Junhui, and Toyoki Kunitake. "Preparation and thermal stability of gold nanoparticles in silk-templated porous filaments of titania and zirconia."*Chemistry of materials* 16.13 (2004): 2656-2661.

[9] Dai, Wei-Lin, Yong Cao, Li-Ping Ren, Xin-Li Yang, Jian-Hua Xu, He-Xing Li, He-Yong He, and Kang-Nian Fan. "Ag–SiO_2–Al_2O_3 composite as highly

active catalyst for the formation of formaldehyde from the partial oxidation of methanol." *Journal of Catalysis* 228.1 (2004): 80-91.

[10] Guo, Yu, Lu Zhou, Wen Zhao, Jian Chen, Makoto Sakurai, Hideo Kameyama. "Effect of Ru and Pt Addition over Plate-type Catalysts for Methane Steam Reforming during Daily Start-up and Shut-down." *Chemistry Letters* 40.2 (2011): 201-203.

[11] Dan, Monica, Maria Mihet, Alexandru R. Biris, Petru Marginean, Valer Almasan, George Borodi, Fumiya Watanabe, Mihaela D. Lazar, and Alexandru S. Biris. "Supported nickel catalysts for low temperature methane steam reforming: comparison between metal additives and support modification." *Reaction Kinetics, Mechanisms and Catalysis* 105.1 (2012): 173-193.

[12] Chang, Feg-Wen, L. Selva Roselin, and Ti-Cheng Ou. "Hydrogen production by partial oxidation of methanol over bimetallic Au–Ru/Fe$_2$O$_3$ catalysts." *Applied Catalysis A: General* 334.1 (2008): 147-155.

[13] Chang, Feg-Wen, Ti-Cheng Ou, L. Selva Roselin, Wun-Syong Chen, Szu Chia Lai, and Hsiao-Min Wu, "Production of hydrogen by partial oxidation of methanol over bimetallic Au–Cu/TiO$_2$–Fe$_2$O$_3$ catalysts," *Journal of Molecular Catalysis A: Chemical* 313 (2009) 55-64.

[14] Shah, Naresh, Devadas Panjala, and Gerald P. Huffman. "Hydrogen production by catalytic decomposition of methane." *Energy & Fuels* 15.6 2001): 1528-1534.

[15] Dusi, Marco, Tamas Mallat, and Alfons Baiker. "Epoxidation of functionalized olefins over solid catalysts." *Catalysis Reviews* 42.1-2 (2000): 213-278.

[16] Dai, Maohua, Dingliang Tang, Zhijie Lin, Hongwei Yang and Youzhu Yuan, "Ti–Si Mixed Oxides by Non-hydrolytic Sol–Gel Synthesis as Potential Gold Catalyst Supports for Gas-phase Epoxidation of Propylene in H_2 and O_2," *Chemistry Letters* 35.8 (2006): 878-879.

[17] Caetano, B. L., L.A. Rocha, E. Molina, Z.N. Rocha, G. Ricci, P.S. Calefi, O.J. de Lima, C. Mello, E.J. Nasser and K.J. Ciuffi, "Cobalt aluminum silicate complexes prepared by the non-hydrolytic sol–gel route and their catalytic activity in hydrocarbon oxidation," *Applied Catalysis A: General* 311 (2006): 122-134.

[18] Dandan Lin, Hui Wu, Rui Zhang and Wei Pan, "Enhanced photocatalysis of electrospun Ag− ZnO heterostructured nanofibers." *Chemistry of Materials* 21.15 (2009): 3479-3484.

[19] Wen, Yanyuan, Hanming Ding, and Yongkui Shan. "Preparation and visible light photocatalytic activity of Ag/TiO_2/graphene nanocomposite." *Nanoscale* 3.10 (2011): 4411-4417.

[20] Ganduglia-Pirovano, M. Verónica, Alexander Hofmann, and Joachim Sauer. "Oxygen vacancies in transition metal and rare earth oxides: Current state of understanding and remaining challenges." *Surface Science Reports* 62.6 (2007): 219-270.

[21] I. M. Tiginyanu, O.Luoan, V. V. Ursaki, L. Chow and M. Enachi."Nanostructures of Metal Oxides." Roberto Fornari. *Comprehensive Semiconductor Science and Technology*. Elsevier, Oxford. 2011, 397-405.

[22] Sreelekha Benny. *High Temperature Water Gas Shift Catalysts: A Computer Modelling Study*. PhD Diss, University College London (United Kingdom), March 2010. [Softcopy]

[23] Belkouch, Jamal, Aïssa Ould-Dris, and Bechara Taouk. "Removal of hazardous chlorinated VOCs over Mn–Cu mixed oxide based catalyst." *Journal of hazardous materials* 169.1 (2009): 758-765.

[24] Routray, Kamalakanta, Laura E. Briand, and Israel E. Wachs. "Is there a relationship between the M=O bond length (strength) of bulk mixed metal oxides and their catalytic activity?." *Journal of Catalysis* 256.1 (2008): 145-153.

[25] Seyed Mahdi Mousavi , Aligholi Niaei , Maria Jose Illan Gomez , Dariush Salari, Parvaneh Nakhostin Panahi and Vicente Abaladejo-Fuentes, "Characterization and activity of alkaline earth metals loaded CeO_2-MO_x (M=Mn, Fe) mixed oxides in catalytic reduction of NO," *Materials Chemistry and Physics* 143.3 (2014): 921-928

[26] Qi, Gongshin, and Wei Li. "NO oxidation to NO_2 over manganese-cerium mixed oxides." *Catalysis Today* 258 (2015): 205-213.

[27] Khaleel, Abbas, Ali Al-Marzouqi, "Alkoxide-free sol–gel synthesis of aerogel iron–chromium mixed oxides with unique textural properties." *Materials Letters* 68 (2012): 385-387.

[28] Chiara Gionco , Alfio Battiato , Ettore Vittone , Maria Cristina Paganini and Elio Giamello, "Structural and spectroscopic properties of high temperature prepared ZrO_2-TiO_2 mixed oxides," *Journal of Solid State Chemistry* 201 (2013): 222-228.

[29] Soylu, Asli Melike , Meryem Polat , Deniz Altunoz Erdogan , Zafer Say , Cansu Yildirim , Ozgur Birer and Emrah Ozensoy, "TiO_2–Al_2O_3 binary mixed oxide surfaces for photocatalytic NO_x abatement." *Applied Surface Science* 318 (2014): 142-149.

[30] Pal, Bonamali, Maheshwar Sharon, and Gyoichi Nogami. "Preparation and characterization of TiO_2/Fe_2O_3 binary mixed oxides and its photocatalytic properties." *Materials Chemistry and Physics* 59.3 (1999): 254-261.

[31] Mora, Enrique Sanchez , Estela Gomez Barojas , Esmeralda Rojas Rojas and Rutilo Silva Gonzalez, "Morphological, optical and photocatalytic properties of TiO_2–Fe_2O_3 multilayers." *Solar energy materials and solar cells* 91.15 (2007): 1412-1415

[32] Mohammadi, M. R., and D. J. Fray. "Low temperature nanocrystalline TiO_2–Fe_2O_3 mixed oxide by a particulate sol–gel route: Physical and sensing characteristics." *Physica E: Low-dimensional Systems and Nanostructures* 46 (2012): 43-51.

[33] Wang, Shaobin, H. M. Ang, and Moses O. Tade. "Volatile organic compounds in indoor environment and photocatalytic oxidation: state of the art." *Environment international* 33.5 (2007): 694-705.

[34] Debecker, Damien P. , Karim Bouchmella , Romain Delaigle , Pierre Eloy , Claude Poleunis , Patrick Bertand , Eric M. Gaigneaux and P. Hubert Mutin, "One-step non-hydrolytic sol–gel preparation of efficient V_2O_5-TiO_2 catalysts for VOC total oxidation." *Applied Catalysis B: Environmental* 94.1 (2010): 38-45.

[35] Zou, Linda, Yonggang Luo , Martin Hooper , Eric Hu ,"Removal of VOCs by photocatalysis process using adsorption enhanced TiO_2–SiO_2 catalyst." *Chemical Engineering and Processing: Process Intensification* 45.11 (2006): 959-964.

[36] Hu, Chaoquan , Qingshan Zhu , Zheng Jiang , Yayuan Zhang andYong Wang, "Preparation and formation mechanism of mesoporous CuO–CeO_2 mixed

oxides with excellent catalytic performance for removal of VOCs." *Microporous and Mesoporous Materials* 113.1 (2008): 427-434

[37] Zeng, Junlin, Xiaolong Liu , Jian Wang , Hanlei , Tingyu Zhu, "Catalytic oxidation of benzene over MnO_x/TiO_2 catalysts and the mechanism study." *Journal of Molecular Catalysis A: Chemical* 408 (2015): 221-227.

[38] Wang, Zhen, Genli Shaen, Jiaqi Li, Haidi Liu, Qi Wang and Yunfa Chen, "Catalytic removal of benzene over CeO_2–MnO_x composite oxides prepared by hydrothermal method." *Applied Catalysis B: Environmental* 138 (2013): 253-259.

[39] Einaga, Hisahiro, Nanako Maeda, and Yasutake Teraoka. "Effect of catalyst composition and preparation conditions on catalytic properties of unsupported manganese oxides for benzene oxidation with ozone." *Applied Catalysis B: Environmental* 142 (2013): 406-413.

[40] Wachs, Israel E., and Kamalakanta Routray. "Catalysis science of bulk mixed oxides." *ACS Catalysis* 2.6 (2012): 1235-1246.

[41] Wachs, Israel E. "Recent conceptual advances in the catalysis science of mixed metal oxide catalytic materials." *Catalysis Today* 100.1 (2005): 79-94.

[42] Wu, Weiyi, Zhao-Hong Huang, and Teik-Thye Lim. "Recent development of mixed metal oxide anodes for electrochemical oxidation of organic pollutants in water." *Applied Catalysis A: General* 480 (2014): 58-78.

[43] Tanaka, Masashi, I. Suh, H. Takada and M. Iwamoto. "Preparation of porous MTiOx (M= Cr, Mo, or W) composite oxides from a mesostructured material of titanium oxysulfate and surfactant micelles based on a wall ion exchange calcination method."*Microporous and Mesoporous Materials* 203 (2015): 274-281.

[44] Xiao, Jiadong, Y. Xie, H. Cao, F. Nawaz, S. Zhang and Y. Wang. "Disparate roles of doped metal ions in promoting surface oxidation of TiO_2 photocatalysis." *Journal of Photochemistry and Photobiology A: Chemistry* 315 (2016): 59-66.

[45] Wang, Ting, G. Yang, J. Liu, B. Yang, S. Ding, Z. Yan and T. Xiao. "Orthogonal synthesis, structural characteristics, and enhanced visible-light photocatalysis of mesoporous Fe_2O_3/TiO_2 heterostructured microspheres." *Applied Surface Science* 311 (2014): 314-323.

[46] Medvedev, A. Ya. "Synthetic armalcolite and pseudobrookite." *Mineralogical Magazine* 60.399 (1996): 347-354.

[47] Neri, G., G. Rizzo, S. Galvagno, G. Loiacono, A. Donato, M.G. Musolino, R. Pietropaolo and E. Rombi, "Sol–gel synthesis, characterization and catalytic properties of Fe–Ti mixed oxides." *Applied Catalysis A: General* 274.1 (2004): 243-251.

[48] Pal, Bonamali, Tomohiro Hata, Kouichi Goto and Gyoichi Nogami. "Photocatalytic degradation of o-cresol sensitized by iron–titania binary photocatalysts." *Journal of Molecular Catalysis A: Chemical* 169.1 (2001): 147-155.

[49] Khaleel, Abbas, and Aysha Al-Nayli. "Supported and mixed oxide catalysts based on iron and titanium for the oxidative decomposition of chlorobenzene. "*Applied Catalysis B: Environmental* 80.1 (2008): 176-184.

[50] Khaleel, Abbas. "Sol–gel synthesis, characterization, and catalytic activity of Fe (III) titanates." *Colloids and Surfaces A: Physicochemical and Engineering Aspects* 346.1 (2009): 130-137.

[51] Li, Rong, Y. Jia, N. Bu, J. Wu and Q. Zhen, "Photocatalytic degradation of methyl blue using Fe_2O_3/TiO_2 composite ceramics." *Journal of Alloys and Compounds* 643 (2015): 88-93.

[52] Guo, W. Q., S. Malus, D.H. Ryan and Z. Altounian."Crystal structure and cation distributions in the $FeTi_2O_5$-Fe_2TiO_5 solid solution series." *Journal of Physics: Condensed Matter* 11.33 (1999): 6337.

[53] Morgado, Edisson, B.A. Marinkovic, P.M Jardim, M.A.S. de Abreu, M. Rocha and P. Bargiela."Studies on Fe-modified nanostructured trititanates."*Materials Chemistry and Physics* 126.1 (2011): 118-127.

[54] Fu, Xiao, Yao Wang, and Fei Wei. "Low Temperature Phase Transition of Ilmenite during Oxidation by Chlorine." *Materials transactions* 50.8 (2009): 2073-2078.

[55] Khaleel, Abbas, and Muhammad Nawaz. "The effect of composition and gel treatment conditions on the textural properties, reducibility, and catalytic activity of sol–gel-prepared Fe (III)–Cr (III) bulk mixed oxides." *Colloids and Surfaces A: Physicochemical and Engineering Aspects* 488 (2016): 52-57.

[56] Cui, Hongtao, Yan Liu, and Wanzhong Ren. "Structure switch between α-Fe_2O_3, γ-Fe_2O_3 and Fe_3O_4 during the large scale and low temperature sol-gel synthesis of nearly monodispersed iron oxide nanoparticles." *Adv Powder Technol* 24.1 (2013): 93-97.

[57] Baumann, Theodore F., Alexander E. Gash, and Joe H. Satcher Jr. "A Robust Approach to Inorganic Aerogels: The Use of Epoxides in Sol–Gel Synthesis."*Aerogels Handbook*. Springer New York, 2011. 155-170.

98

[58] Morterra, Claudio, and Giuliana Magnacca. "A case study: surface chemistry and surface structure of catalytic aluminas, as studied by vibrational spectroscopy of adsorbed species." *Catalysis Today* 27.3 (1996): 497-532.

[59] Oiamo, Tor H., M. Johnson, K. Tang and I.N. Luginaah."Assessing traffic and industrial contributions to ambient nitrogen dioxide and volatile organic compounds in a low pollution urban environment." *Science of The Total Environment* 529 (2015): 149-157.

[60] Zhao, Yan, Wenjing Lu, and Hongtao Wang. "Volatile trace compounds released from municipal solid waste at the transfer stage: evaluation of environmental impacts and odour pollution." *Journal of hazardous materials* 300 (2015): 695-701.

[61] Huang, Binbin, C. Lei, C. Wei and G. Zeng."Chlorinated volatile organic compounds (Cl-VOCs) in environment—sources, potential human health impacts, and current remediation technologies." *Environment international* 71 (2014): 118-138.

[62] Zhang, Zhixiang, Zheng Jiang, and Wenfeng Shangguan. "Low-temperature catalysis for VOCs removal in technology and application: A state-of-the-art review." *Catalysis Today* (2015).

[63] Li, W. B., J. X. Wang, and H. Gong. "Catalytic combustion of VOCs on non-metal catalysts." *Catalysis Today* 148.1 (2009): 81-87.

[64] Das, D. P., and K. M. Parida. "Mn (III) oxide pillared titanium phosphate (TiP) for catalytic deep oxidation of VOCs." *Applied Catalysis A: General* 324 (2007): 1-8.

[65] Tabakova, T., D. Dimitrov, M. Manzoli, F. Vindigni, P. Petrova, L. Ilieva, R. Zanella, and K. Ivanov. "Impact of metal doping on the activity of Au/CeO 2

catalysts for catalytic abatement of VOCs and CO in waste gases." *Catalysis Communications* 35 (2013): 51-58.

[66] Zhou, Guilin, Xiaoling He, Shnf. Liu, Hongmei Xie, and Min Fu. "Phenyl VOCs catalytic combustion on supported CoMn/AC oxide catalyst." *Journal of Industrial and Engineering Chemistry* 21 (2015): 932-941.

[67] Piumetti, Marco, Debora Fino, and Nunzio Russo. "Mesoporous manganese oxides prepared by solution combustion synthesis as catalysts for the total oxidation of VOCs." *Applied Catalysis B: Environmental* 163 (2015): 277-287.

[68] Khaleel, Abbas. "Sol–gel synthesis, characterization, and catalytic activity of Fe (III) titanates." *Colloids and Surfaces A: Physicochemical and Engineering Aspects* 346.1 (2009): 130-137.

[69] Li, Rong, Y. Jia, N. Bu, J. Wu, and Q. Zhen. "Photocatalytic degradation of methyl blue using Fe_2O_3/TiO_2 composite ceramics." *Journal of Alloys and Compounds* 643 (2015): 88-93.

[70] Wachs, Israel E. "Recent conceptual advances in the catalysis science of mixed metal oxide catalytic materials." *Catalysis Today* 100.1 (2005): 79-94.

[71] Xiao, Jiadong, Y. Xie, H. Cao, F. Nawaz, S. Zhang, and Y. Wang. "Disparate roles of doped metal ions in promoting surface oxidation of TiO_2 photocatalysis." *Journal of Photochemistry and Photobiology A: Chemistry* 315 (2016): 59-66..

[72] Wang, Ting, G. Yang, J. Liu, B. Yang, S. Ding, Z. Yan, and T. Xiao. "Orthogonal synthesis, structural characteristics, and enhanced visible-light photocatalysis of mesoporous Fe_2O_3/TiO_2 heterostructured microspheres." *Applied Surface Science* 311 (2014): 314-323.

[73] Khaleel, Abbas, and Aysha Al-Nayli. "Supported and mixed oxide catalysts based on iron and titanium for the oxidative decomposition of chlorobenzene."*Applied Catalysis B: Environmental* 80.1 (2008): 176-184.

[74] Guo, W. Q., S. Malus, D.H. Ryan, and Z. Altounian. "Crystal structure and cation distributions in the FeTi2O5-Fe2TiO5 solid solution series." *Journal of Physics: Condensed Matter* 11.33 (1999): 6337.

[75] Morgado, Edisson, B.A. Marinkovic, P.M Jardim, M.A.S. de Abreu, M. Rocha, and P. Bargiela."Studies on Fe-modified nanostructured trititanates."*Materials Chemistry and Physics* 126.1 (2011): 118-127.

[76] Fu, Xiao, Yao Wang, and Fei Wei. "Low Temperature Phase Transition of Ilmenite during Oxidation by Chlorine." *Materials transactions* 50.8 (2009): 2073-2078.

[77] Guczi, Laszlo, Goran Boskovic, and Ernő Kiss. "Bimetallic cobalt based catalysts." *Catalysis Reviews: Science and Engineering* 52.2 (2010): 133-203.

[78] Chen, Li-Chung, and Shawn D. Lin. "The ethanol steam reforming over Cu-Ni/SiO_2 catalysts: Effect of Cu/Ni ratio." *Applied Catalysis B: Environmental* 106.3 (2011): 639-649.

[79] Morales, María Roxana, Bibiana P. Barbero, and Luis E. Cadús. "Evaluation and characterization of Mn–Cu mixed oxide catalysts for ethanol total oxidation: influence of copper content." *Fuel* 87.7 (2008): 1177-1186.

[80] Fierro, V., O. Akdim, H. Provendier and C. Mirodatos, "Ethanol oxidative steam reforming over Ni-based catalysts."*Journal of Power Sources* 145.2 (2005): 659-666

[81] Latorre, N., F. Gazana, V. Martineez-Hansen, C. Royo, E. Romeo and A. Monzon, "Ni-Co-Mg-Al catalysts for hydrogen and carbonaceous

nanomaterials production by CCVD of methane." *Catalysis today* 172.1 (2011): 143-151.

[82] H.P. Wulff, F. Wattinmena, U.S. Patent 4,367,345 (1983).

[48] Sachse, Alexander, V. Hulea, K.L, Kostov, N. Marcotte, M.Y. Boltoeva, E. Belamie and B. Alonso, "Efficient mesoporous silica–titania catalysts from colloidal self-assembly." *Chemical Communications* 48.86 (2012): 10648-10650.

[83] Lafond, V., P. H. Mutin, and A. Vioux. "Non-hydrolytic sol–gel routes based on alkyl halide elimination: toward better mixed oxide catalysts and new supports: application to the preparation of a SiO_2–TiO_2 epoxidation catalyst." *Journal of Molecular Catalysis A: Chemical* 182 (2002): 81-88.

[84] V. V. Hong, Amorphous TiO_2 nanoparticles : Review, Chemical Physical Research Journal, 4 (2011) 43-62.

[85] G. Cappelletti, TiO_2 nanoparticles: Traditional and novel synthetic method for photocatalytic paint formulation, A. E. Kestekk, G. T. DeLorey (Eds.), Nanoparticles, Nova Science Publishers, 2010, pp. 213-254.

[86] Huang, Jing , Shurong Wang , Yingqiang Zhao , Xiaoying Wang , Shuping Wang , Shihua Wu , Shoumin Zhang , Weiping Huang, "Synthesis and characterization of CuO/TiO_2 catalysts for low-temperature CO oxidation." *Catalysis Communications* 7.12 (2006): 1029-1034.

[87] Meshal K. Al-Dihani, Sami H. Ali, Jamal N. Al-Saeedi."Synthesis & Characterization of Nano-Crystalline Bulk Mixed Oxides Catalysts", 15th Annul Soudi-Japan Symposium, KFUPM, Dhahran, KSA December 7-8, 2015.

[88] Sales, Emerson Andrade, B, Benhamida, V, Caizergues, J,-P. Lagier, F. Fievet and F. Bozon- Verduraz. "Alumina-supported Pd, Ag and Pd–Ag catalysts: preparation through the polyol process, characterization and reactivity in hexa-1, 5-diene hydrogenation." *Applied Catalysis A: General*172.2 (1998): 273-283.